EUROPEAN RESPIRATORY *journal*

FLAGSHIP SCIENTIFIC JOURNAL OF ERS

Early View

Original research article

Nicotine promotes e-cigarette vapour-induced lung inflammation and structural alterations

Elsa T. Roxlau, Oleg Pak, Stefan Hadzic, Claudia F. Garcia-Castro, Marija Gredic, Cheng-Yu Wu, Julia Schäffer, Balachandar Selvakumar, Alexandra Pichl, David Spiegelberg, Janik Deutscher, Mariola Bednorz, Katharina Schäfer, Simone Kraut, Djuro Kosanovic, Esraa M Zeidan, Baktybek Kojonazarov, Susanne Herold, Ievgen Strielkov, Andreas Guenther, Jochen Wilhelm, Mohamed M. A. Khalifa, Ashraf Taye, Ralf P. Brandes, Matthias Hecker, Friedrich Grimminger, Hossein A. Ghofrani, Ralph T. Schermuly, Werner Seeger, Natascha Sommer, Norbert Weissmann

Please cite this article as: Roxlau ET, Pak O, Hadzic S, *et al*. Nicotine promotes e-cigarette vapour-induced lung inflammation and structural alterations. *Eur Respir J* 2023; in press (https://doi.org/10.1183/13993003.00951-2022).

Nicotine promotes e-cigarette vapour-induced lung inflammation and structural alterations

Elsa T. Roxlau[1*§], Oleg Pak[1*], Stefan Hadzic[1], Claudia F. Garcia-Castro[1], Marija Gredic[1], Cheng-Yu Wu[1], Julia Schäffer[1], Balachandar Selvakumar[1,2], Alexandra Pichl[1], David Spiegelberg[1], Janik Deutscher[1], Mariola Bednorz[1], Katharina Schäfer[1], Simone Kraut[1], Djuro Kosanovic[1,3], Esraa M Zeidan[1,4], Baktybek Kojonazarov[1,5], Susanne Herold[1], Ievgen Strielkov[1], Andreas Guenther[1], Jochen Wilhelm[1,5], Mohamed M. A. Khalifa[4], Ashraf Taye[6], Ralf P. Brandes[7], Matthias Hecker[1], Friedrich Grimminger[1], Hossein A. Ghofrani[1,8], Ralph T. Schermuly[1], Werner Seeger[1,5,9], Natascha Sommer[1&], Norbert Weissmann[1]

[1]Justus Liebig University, Excellence Cluster Cardio-Pulmonary Institute (CPI), Universities of Giessen and Marburg Lung Center (UGMLC), Member of the German Center for Lung Research (DZL), Giessen, Germany

[2]Sharjah Institute of Medical Research (SIMR), College of Medicine- University of Sharjah (UoS), Sharjah, United Arab Emirates.

[3]I.M. Sechenov First Moscow State Medical University (Sechenov University), Moscow, Russia

[4]Department of Pharmacology and Toxicology, Faculty of Pharmacy, Minia University, El-Minia, Egypt.

[5]Institute for Lung Health (ILH), Giessen, Germany

[6]Department of Pharmacology and Toxicology, Faculty of Pharmacy, South Valley University, Egypt

[7]Institute for Cardiovascular Physiology, Goethe University, Cardio-Pulmonary Institute (CPI), Frankfurt, Germany.

[8]Department of Medicine, Imperial College London, London, United Kingdom

[9]Max Planck Institute for Heart and Lung Research, Bad Nauheim, Germany

* Shared position

§ Portions of the doctoral thesis of Elsa T. Roxlau are incorporated into this report

& Corresponding author

Corresponding Author: Natascha Sommer
Natascha.Sommer@innere.med.uni-giessen.de
Address: Aulweg 130, 35392 Giessen, Germany
Phone number: +49 641/99-42471, Fax number: +49 641/99-42419

Word counts: 3988

Take home message:

E-cigarette use, particularly with nicotine-containing vapour, is a harmful alternative to tobacco smoking. Nicotine-containing e-cigarette vapour increased pulmonary endothelial permeability, induced inflammation and caused mild airway and parenchymal alterations.

Abstract

Electronic cigarette (e-cigarette) vapour is gaining popularity as an alternative to tobacco smoking and can induce acute lung injury. However, the specific role of nicotine in e-cigarette vapour and its long-term effects on the airways, lung parenchyma and vasculature remain unclear. We found that *in vitro* exposure to nicotine-containing e-cigarette vapour extract (ECVE) or nicotine-free extract (NF ECVE) induced changes in gene expression of epithelial cells and pulmonary arterial smooth muscle cells (PASMC), but preferentially ECVE caused functional alterations (e.g. decrease of human or mouse PASMC proliferation by 29.3±5.3% or 44.3±8.4%, respectively). Additionally, acute inhalation of nicotine-containing e-cigarette vapour (ECV) but not nicotine-free vapour (NF ECV) increased pulmonary endothelial permeability in isolated lungs. Long-term, *in vivo* exposure of mice to ECV for 8 months significantly increased the number of inflammatory cells, in particular lymphocytes compared to control and NF ECV in the bronchoalveolar lavage (BAL, ECV: 853.4±150.8, control: 37.0±21.1, NF ECV: 198.6±94.9 cells/ml) and in lung tissue (ECV: 25.7±3.3, control: 4.8±1.1, NF ECV: 14.1±2.2 cells/mm^3). BAL-cytokines were predominantly increased by ECV. Moreover, ECV caused significant changes in lung structure and function (e.g. increase in airspace by 17.5±1.4% compared to control), similar to mild tobacco smoke-induced alterations, which also could be detected in the NF ECV group, albeit to a lesser degree. In contrast, the pulmonary vasculature was not significantly affected by ECV or NF ECV. In conclusion, NF ECV components induce cell-type specific effects and mild pulmonary alterations, while inclusion of nicotine induces significant endothelial damage, inflammation and parenchymal alterations.

Introduction

Chronic exposure to cigarette smoke (CS) is a major trigger of chronic obstructive pulmonary disease (COPD), which affects more than 174 million people worldwide [1]. COPD comprises pulmonary inflammation, airway obstruction, pulmonary emphysema and often pulmonary hypertension (PH) [2]. Aside from nicotine, numerous ingredients in tobacco smoke are responsible for increased oxidative stress and activation of immune cells, leading to airway destruction and chronic inflammation in the lung [3]. Therefore, the substitution of traditional tobacco smoking with electronic cigarettes (e-cigarettes) containing liquids that optionally include nicotine and/or different flavours to produce an aerosol (commonly referred to as vapour or e-cigarette vapour) for inhalation has grown in popularity as a healthier alternative to cigarette smoking, especially among young people [4].

Despite a growing number of studies in this area, there is currently no consensus on the effects of e-cigarette smoking on human health. The large variability of e-liquid content (e.g. flavours, nicotine), technical specifications of e-cigarettes (e.g. voltage, temperature) and user habits (e.g. puff duration, number of puffs), and the relatively short period that e-cigarettes have been in use hamper robust scientific conclusions, in particular, those concerning their long-term effects [5]. Accordingly, studies in humans reported discrepant results with a decrease [6], an increase [7] or no change [8] of inflammatory markers after short-term use of e-cigarettes. Moreover, although until recently, studies in humans did not find severe effects of e-cigarette use on health [5], more than 2600 cases of acute e-cigarette or vaping-product-associated lung injury (EVALI) have been reported in recent years [9].

Due to these variabilities and limited experience with long-term effect in humans, it is necessary to assess the effects of e-cigarette vapour in a clearly-defined animal model. Previously, discrepant results from *in vivo* studies concerning the development of CS-

like lung structural alterations, such as emphysema, have been reported; some studies show signs of emphysema after 4 months [10], and others demonstrate no effect after 8 months [11] of exposure to nicotine-containing *(*18mg/ml) e-cigarette vapour. Furthermore, cell type-specific effects on primary lung cells and the impacts of e-cigarette vapour on pulmonary vasculature remain to be addressed in research. In this regard, previous *in vitro* experiments suggested cell type specific cytotoxic effects of different e-cigarette preparations depending on their ingredients [12-16].

Therefore, we investigated 1) the *in vitro* effects of nicotine-containing e-cigarette vapour extract (subsequently termed ECVE) and nicotine-free e-cigarette vapour extract (subsequently termed NF ECVE) on different human and murine pulmonary cell types, 2) the short-term *ex vivo* effects of e-cigarette vapour with nicotine (ECV) and without nicotine (NF ECV) on endothelial permeability in isolated perfused and ventilated mouse lungs, and 3) the long-term *in vivo* effects of ECV and NF ECV on pulmonary function, structure and the vasculature.

Methods

For detailed methods, please see the online supplementary material.

Animal experiments

Wild-type C57BL/6J mice were obtained from Charles River Laboratories (Sulzfeld, Germany). Animals were housed under controlled conditions of a 14/10 daylight/night cycle with food and water supply *ad libitum*. All experiments were approved by the governmental ethics committee for animal welfare (Regierungspräsidium Giessen, Germany, GI 20/10, Nr. 105/2014, GI 20/10, Nr. 74/2016, GI 20/10, Nr. 115/2014).

Cell culture

Primary mATII cells were isolated, as described previously, by negative selection of CD16/32+ (553142, BD Biosciences, Franklin Lakes, USA) and CD45+ cells (553076, BD Biosciences, Franklin Lakes, USA) [17]. Primary mPASMC were isolated from precapillary pulmonary arterial vessels as described previously [18]. Primary hPASMC were isolated from pulmonary arteries of donor lung transplants by dissection of the medial layer. The studies with hPASMC were approved by the Ethics Committee of the Faculty of Medicine at Justus-Liebig University Giessen (AZ 58/15, AZ 10/06). A549 cells were purchased from the German Collection of Microorganisms and Cell Cultures (DSMZ, Braunschweig, Germany) and human bronchial epithelial cells (HBEpC) from PromoCell (Heidelberg, Germany). All cells were cultured in a humidified atmosphere of 5% CO_2 at 37°C in a cell incubator. 24h after seeding, the cell culture medium was replaced with a medium containing different doses of ECVE, NF ECVE or CS extract (CSE) (for preparation, see below). The medium bubbled with room air served as the control medium. For detailed isolation protocols and functional assays, please refer to the supplementary material.

Preparation of ECVE and CSE for *in vitro* assays

100% ECVE or NF ECVE was produced by bubbling the vapour from an e-cigarette (2.2Ohm, 3.3V, Joyetech eGo-C, Shenzhen, China) filled with 0.8ml e-cigarette liquid (60% propylene glycol, 30% glycerol and 10% water; Riccardo Retail GmbH, Neubrandenburg, Germany) either containing 18mg/ml nicotine or without nicotine through 10ml of culture medium. The puffing condition was 15 puffs of 4 sec duration and 20 sec intervals between them. 100% CSE was freshly prepared by bubbling 10ml of basal cell culture medium (without foetal calf serum) with mainstream smoke of one 3R4F cigarette (University of Kentucky, Lexington, USA). After pH adjustment to 7.4, the medium was sterile-filtered through a 0.22µm pore filter, and the CSE

concentration was determined spectrophotometrically (absorbance 290nm). For control experiments, 100% medium for the respective cell type was bubbled with room air for 5 min.

E-cigarette vapour application in the isolated ventilated and perfused mouse lung system

The isolated ventilated and perfused mouse lung system was used to investigate the effects of repetitive intra-tracheal application of ECV and NF ECV on hypoxic pulmonary vasoconstriction (HPV) and the capillary filtration coefficient (K_{fc}) [19]. A detailed description is provided within the supplementary material.

Animals and e-cigarette vapour exposure

To generate e-cigarette vapour for animal exposure, Joyetech eVic-VTC Mini e-cigarettes (coil resistance: 0.15Ohm, 4.1V, 15-50W, Joyetech, Riccardo Retail GmbH, Neubrandenburg, Germany) were integrated into a custom made “inExpose” inhalation exposure chamber (SCIREQ Scientific Respiratory Equipment Inc., Montreal, Canada). This automated system (FlexiWare 6.1, SCIREQ Scientific Respiratory Equipment Inc., Montreal, Canada) was set to inject one 60ml puff per min with a flow of 3l/min into the whole-body exposure chamber. Mice were randomly allocated to the control group or the ECV or NF ECV exposure groups for 6 h/day, 5 days/week for 8 months. Control animals were housed under otherwise identic conditions to those of the ECV/NF ECV-exposed mice and were age- and sex-matched. Commercially available e-liquids [60% propylene glycol (PG), 30% glycerol (VG) and 10% (water) (Avoria GmbH, Nuremberg, Germany] with (18mg/ml) or without (0mg/ml) nicotine or flavouring were used. A MicroDust Pro (UT-CEL712, Casella Measurements, Bedford,

UK) device was integrated into the vapour exposure system for real-time monitoring of aerosols. For conventional CS, the mice were exposed as previously described [17].

In vivo hemodynamics, lung function, micro-CT imaging and echocardiography

Lung function and structure and pulmonary vascular function and structure were determined as described previously [17, 20]. Heart function was measured by transthoracic echocardiography using a VEVO770 or VEVO2100 system (Visualsonics, Toronto, Canada). *In vivo* µCT images were acquired using a Quantum GX microCT scanner (PerkinElmer, Waltham, USA) as previously described [20].

Flow cytometry

Flow cytometry was performed with an LSRII flow cytometer (BD Biosciences, Franklin Lakes, USA) using the DIVA software (BD Biosciences, Franklin Lakes, USA) as previously described [21, 22]. For detailed methods and the gating strategy, please refer to the supplementary material.

Immunohistochemistry

Immunohistochemical staining was performed using 3µm sections of mouse lungs [23]. CD3-positive cells were counted per section area of the lung. CD45-positive cells were counted around vessels, septa and bronchi in randomly selected fields according to the following scale: 0 – small number of CD45+ cells, 1 – moderate number of CD45+ cells, and 2 – many CD45+ cells. A detailed description is provided within the supplementary material.

Multiplex assay

A custom-made mouse magnetic bead-based multiplex assay was used to analyse the levels of selected inflammatory mediators in bronchoalveolar lavage fluid (BALF) according to the manufacturer's protocol (R&D Systems, Minneapolis, USA).

Statistical analysis

Data are reported as mean ± standard error of the mean (SEM). Statistical analyses using Student’s t-test or one-way ANOVA with Tukey’s post-hoc-test were carried out using GraphPad Prism®. The combined p-value of the *in vivo* lung functional measurements was calculated by a meta-analysis using Fisher's method and the 'BisRNA' R package. Categorical analysis was done using pair-wise Wilcoxon tests with continuity correction to evaluate the data from immunohistochemical staining of CD45+ cells. For comparison of the *in vivo* effects of ECV and NF ECV, binominal analysis was performed by using Binom.Dist in Excel. For this analysis, parameters were categorised as alterations either compatible or incompatible with pathological changes seen in smoke-induced emphysema or pulmonary hypertension using differences in mean values of the different parameters.

Results

ECVE and NF ECVE differentially affected metabolic activity and proliferation of murine and human cultured pulmonary cells

High dose NF ECVE treatment decreased metabolic activity in isolated mouse alveolar type II (mATII) cells and A549 cells (Figure 1a, Supplementary Figure 1a), only, while ECVE treatment decreased metabolic activity in all epithelial cell types and human pulmonary arterial smooth muscle cells (hPASMC) at high concentrations (100% ECVE; Figure 1a, d, e, Supplementary Figure 1a). Proliferation of murine and human PASMC at lower concentrations (15% ECVE) that did not affect metabolic activity was also diminished following ECVE but not NF ECVE treatment (Figure 1c, f, Supplementary Figure 1b). Accordingly, only 15% ECVE decreased mouse and human PASMC confluence, without affecting migration or the number of dead cells (Supplementary Figure 1c-g). Moreover, ECVE and NF ECVE did not show any cytotoxic effects at any concentration (Supplementary Figure 2a-e) or induce apoptosis compared to the untreated controls (Supplementary Figure 2f-j). In contrast, exposure to CSE decreased the metabolic activity of all cell types (Figure 1a, b, d, e, Supplementary Figure 1a), decreased cell confluence (Supplementary Figure 1c, d) and migration (Supplementary Figure 1e, f), induced cellular toxicity and increased apoptosis (Supplementary Figure 2a-j). The paradoxical reduction in apoptosis in some of these experiments may be explained by faster action of 100% CSE compared to 50% CSE (Supplementary Figure 2k).

ECVE and NF ECVE exposure changed gene expression patterns in a cell-type-specific manner

Hypothesis-driven and non-hypothesis-driven approaches were used to study the ECVE and NF EVCE effects on signalling pathways in mPASMC and mATII cells. First, the expression levels of different genes, which were changed specifically in vessels and/or septa after *in vivo* cigarette smoke (CS) exposure [24], were investigated in mPASMC and mATII cells. Interestingly, only ECVE but not NF ECVE increased the mRNA expression of inducible nitric oxide synthase (*Nos2)* and cyclin A1 (*Ccna1)* specifically in mPASMC (Supplementary Figures 3a-b). Second, microarray analysis of ECVE and NF ECVE treated mATII, and mPASMC revealed cell type-specific alterations of various pathways in these cells, largely independent of the presence of nicotine in the vapour extract (Figure 2a, b, Supplementary Figures 3c-f, 4a-i and 5a-j). The most consistently regulated genes after exposure to either ECVE or NF ECVE were an upregulation of DAZ interacting protein 1-like (*Dzip1l*) in mATII and a downregulation of UDP-N-acetylglucosamine pyrophosphorylase 1-like 1 (*Uap1l1*) and dipeptidyl peptidase 7 (*Dpp7*) in mPASMC (Supplementary Figures 3c-f). Besides a general effect on metabolic pathways, we found specific upregulation of glutathione metabolism in mATII cells (Figure 2a) and downregulation of the lysosomal pathways in mPASMC (Figure 2b). We confirmed these results by showing that the ratio of GSH/GSSG was decreased by the application of ECVE or NF ECVE in mATII cells (Figure 2c) and that protein expression levels of markers of the autophagy-lysosome system, microtubule-associated proteins 1A/1B light chain 3B (LC3-II) and p62, were decreased in mPASMC (Figure 2d).

ECV and NF ECV inhalation increased endothelial permeability

To investigate the effects of ECV and NF ECV on HPV and endothelial permeability, we used an isolated perfused and ventilated mouse lung model. Repetitive application of ECV or NF ECV via the trachea attenuated HPV in both the ECV and NF ECV

groups (Figure 3a). However, only the inhalation of ECV (but not of NF ECV) increased the capillary filtration coefficient (Kf_c) as a measure of endothelial permeability (Figure 3b).

Long-term exposure to ECV caused a pulmonary inflammatory response

To evaluate the immune response of the lung to ECV and NF ECV exposure, flow cytometry of BAL and multiplex immunoassay analysis of BALF (i.e., BAL supernatant) from mice exposed to NF ECV or ECV for 8 months were performed (Figure 4). The flow cytometry gating strategy is depicted in Supplementary Figure 6a. Although there was only a trend toward an increase in the total number of cells in BAL from mice exposed to ECV (Figure 4a), there was a significant increase in the number of neutrophils (Figure 4b, Supplementary Figure 6b) and lymphocytes (Figure 4c, Supplementary Figure 6b). Moreover, despite an unchanged number of total macrophages after ECV or NF ECV exposure (Figure 4d), only ECV significantly shifted the macrophage population from resident macrophages (rAM) to pro-inflammatory exudative macrophages (ExMAs; Figure 4 e-f, Supplementary Figure 6b); NF ECV had no such effect.

Multiplex screening of selected inflammatory mediators in BALF showed that ECV altered the levels of chemokine (C-C motif) ligands (CCL) in BALF (Figure $4g_i$). ECV decreased CCL3 while it increased CCL8 and CCL12 levels, indicating a dysbalance of recruitment and activation of different immune cells [25-27]. In addition, only ECV increased the levels of pro-inflammatory interleukins (IL) 5, 13 and 16 (Figure $4g_{ii}$), which promote autoimmune responses as seen in asthma [28], while NF ECV did not. In contrast, ECV exposure decreased the level of IL-2 (Figure $4g_{ii}$), the main driver of T cell proliferation and differentiation, and anti-viral responses [29, 30]. Interestingly,

only NF ECV increased the level of IL-33 (Figure 4g$_{ii}$), which promotes the production of Th2-associated cytokines [31]. Screening of other cytokines and chemokines did not reveal any significant alterations (Supplementary Figure 7a-c). Moreover, we investigated various matrix metalloproteinases (MMP) in BALF, which are known to be associated with increased inflammation in COPD. ECV exposure increased MMP-9 and MMP-12 levels, while NF ECV only increased MMP-12 in BALF from mice exposed to e-cigarette vapour for 8 months (Figure 4g$_{iii}$). Other MMPs did not reveal any significant alterations (Supplementary Figure 7d).

To further investigate the effects of ECV and NF ECV on lymphocytes, which showed a change in the initial screening by FACS but were not characterised in detail, we investigated CD45+ cells (leukocytes) and T cell infiltration (CD3+) in lung sections. Interestingly, the immunohistochemical staining of CD45+ cells revealed that ECV induced a higher accumulation of leukocytes in the different compartments of the lung compared to NF ECV and confirmed the FACS data by showing an increased number of CD3+ T cells in the lung tissue of ECV treated mice compared to NF ECV (Figure 4h-j).

Long-term exposure to ECV resulted in structural and functional pulmonary changes without effects on the lung vasculature

In vivo exposure of mice to ECV in our setup resulted in lower plasma concentrations of nicotine and cotinine compared to conventional CS exposure (nicotine: 3.8±0.9ng/ml vs. 16.0±3.0ng/ml; cotinine: 6.2 ± 0.9ng/ml vs. 50.7±7.4ng/ml; Supplementary Figure 8a-c). During 8 months of exposure, the mice gained weight to a similar level in all experimental groups (Supplementary Figure 8d). The haematocrit (HCT) was increased in mice after exposure to ECV for 8 months (Supplementary Figure 8e).

Lung functional parameters (Figure 5a-d) showed a trend of being affected by ECV. Meta-analysis of p-values from lung function (Figure 5a: static compliance, Figure 5b: resistance and Figure 5c: inspiratory capacity) suggests that ECV induced significant functional alterations similar to CS-induced emphysema-like changes (combined p=0.03); we did not detect significant differences in the NF ECV group. Moreover, only exposure to ECV for 8 months induced significant structural alterations of the pulmonary parenchyma, as determined by *in vivo* µCT imaging (Figure 5e-g) and histological analysis (Figure 5h-j), while NF ECV exposure did not show this result.

In contrast, after long-term exposure of mice to ECV or NF ECV, we did not detect statistically significant alterations indicating induction of PH, which was assessed by hemodynamic measurements and morphological analysis of the pulmonary vasculature (Figure 6a-c). Accordingly, long-term exposure of mice to ECV or NF ECV did not significantly affect the Fulton index (Figure 6d), or right ventricular (RV) or global heart function evaluated by echocardiography (Figure 6e-h). Meta-analysis of p-values also did not indicate any statistically significant effect of ECV or NF ECV on the pulmonary vasculature.

Although no significant effect of NF ECV on single measurement parameters was detected, binominal analysis of parameters characterising the pulmonary airways/parenchyma indicated that in the NF ECV group, the phenotype was more affected compared to the control group and less compared to the ECV group, (Table 1a, b). Furthermore, we detected a significant difference between the NF ECV and ECV groups when performing a combined analysis of the inflammatory and pulmonary airway/parenchymal parameters (combined p=0.031), supporting the notion that nicotine promotes the effects of e-cigarette vapour on inflammation and airway/parenchymal parameters.

Discussion

Our study provides evidence that ECV can induce acute and chronic lung damage. Although both nicotine-containing e-cigarette vapour (ECV) and nicotine-free e-cigarette vapour (NF ECV) affected functional and gene expression patterns in pulmonary cells *in vitro* and airway/parenchymal parameters, only ECV significantly increased endothelial permeability *ex vivo*, and promoted inflammation and mild structural and functional pulmonary alterations *in vivo*, similar to CS-induced alterations after long-term exposure. However, in contrast to CS exposure, we did not detect significant pulmonary vascular alterations.

Our *in vitro* experiments showed that ECVE and NF ECVE reduce metabolic activity in specific cell types only at high concentrations but are insufficient to induce cytotoxic effects or trigger apoptosis. Furthermore, nicotine promotes the inhibitory effects of e-cigarette vapour on metabolic activity and proliferation, the latter at least in PASMC. Due to the lack of general standardisation of e-cigarette vapour generation, comparing other published studies with our data is limited [32]. In this regard, some studies reported no effect (regardless of the nicotine content and flavouring) of the pad-collected e-cigarette extracts in CHO-K1/A549 cells [14], while another observed a dose- and flavour-dependent decrease of CALU3 cell viability after e-cigarette vapour exposure [15]. Despite the more pronounced effect of ECVE on cellular functions, microarray analysis showed that exposure to ECVE and NF ECVE changed gene expression patterns differentially in mATII cells compared to mPASMC but largely independent from nicotine content, suggesting that ECVE and NF ECVE trigger transcriptional alterations with hitherto unknown functional relevance. In line with our microarray data, we showed downregulation of the GSH/GSSG ratio in mATII cells and of two proteins involved in the autophagy-lysosomal pathway, LC3-II (an active lipid-

modified form of LC3) and p62 (autophagy receptor) in mPASMC in a nicotine-independent manner. GSH depletion and decreased GSH/GSSG levels occur in many different cell types secondary to CSE-induced oxidative stress [33, 34]. The relevance of downregulated lysosomal pathway in mATII cells remains unclear; however, previously, alterations of lysosomal pathways were found to contribute to the pathogenesis of COPD [35].

As recently acute respiratory distress syndrome (ARDS) was associated with vaping [36], we investigated the acute effects of ECV inhalation on endothelial permeability in isolated mouse lungs. Interestingly, only ECV but not NF ECV increased capillary permeability, indicating the effect of nicotine. Nicotine could directly alter the function of vascular endothelial cells, PASMC, airway epithelial cells, and immune cells expressing nicotinic acetylcholine receptors [37], thus promoting increased capillary permeability. Although using oil-formulated tetrahydrocannabinol or cannabidiol in ECV was suggested to be associated with vaping-induced ARDS, our data indicate that nicotine in e-cigarettes may contribute to ARDS development [6, 7, 36-39]. Similarly, cigarette smoke increases the risk of ARDS due to alterations in pulmonary vascular permeability and endothelial barrier function [38]. In addition to endothelial permeability, pulmonary vasoreactivity, in response to acute hypoxia, was affected by e-cigarette vapour, independently from the presence of nicotine. This suggests that ECV or NF ECV may alter the endothelial release of vasoactive mediators, as inhaled cigarette smoke reversed human HPV through the NO-cGMP signalling pathway [40].

In accordance with our *ex vivo* studies, *in vivo* ECV or NF ECV treatment for 8 months showed different effects, related to the presence or absence of nicotine. Only exposure to ECV – not NF ECV – resulted in a significant increase of inflammatory cells in the BAL, as well as of CD45+ in different compartments of the lung. However, ECV

exposure showed a significantly higher accumulation of CD3+ T cells in the lungs compared to NF ECV. In this regard, FACS analysis of BAL may be limited, as lymphocytes were only identified by their scattering properties in our study and were not further characterised. Moreover, BALF analysis shows that presence of nicotine enhances recruitment and activation of immune cells such as T cells, eosinophils and macrophages, indicated by increased CCL8 and CCL12 [25-27], and triggers an inflammatory response similar as seen in asthma, indicated by an increase in IL-5 and IL-13 [41, 42], so one could speculate that ECV induces an allergic reaction and predisposes to bronchial hyper-reagibility [28]. In line with our data, previous studies have shown that exposure to nicotine-containing ECV altered lung inflammatory responses in mice after 3 days [43], 2 weeks [44] and 4 months [10] and in humans after 4 weeks [45], leading to macrophage-mediated inflammation [44] and increased levels of pro-inflammatory cytokines [43]. Moreover, the presence of nicotine increased lymphocyte levels in human BAL [44]. Interestingly, in our study, ECV significantly increased MMP-9 and 12 levels in BALF, while NF ECV increased MMP-9 levels only. MMP-9 and -12 are important mediators associated with inflammation and the development of COPD [46, 47]. These findings align with our *in vivo* study, demonstrating a more pronounced effect of ECV than NF ECV on pulmonary structural alterations, which showed characteristics of CS-induced alterations, albeit less pronounced. Previous *in vivo* studies suggested development of emphysema [10], lung functional alterations [48] or no effect [11] of long-term ECV treatment in mice. However, differences in mice strains [10], age of mice [48] and daily duration of ECV exposure [11] may explain discrepancies with regard to severity of development of lung functional and structural alterations.

Plasma nicotine levels of 3.8±0.9ng/ml in our study are comparable to low concentrations in human e-cigarette users. In clinical studies, the levels of nicotine in the plasma of e-cigarette users vary from ~1ng/ml to ~50ng/ml depending on study design, the e-cigarette device *etc.* [49, 50]. Interestingly, a prospective human study over 3.5 years did not find any functional or structural changes in 9 subjects that used e-cigarettes daily [51]; however, the exposure time is much lower compared to the mouse model. Moreover, from our study, we cannot exclude a harmful effect of NF ECV, as we found in the distribution analysis of pathological values an effect of NF ECV compared to control. However, we did not find a statistically significant difference for single parameters.

In contrast to lung functional, airway and alveolar alterations, we did not detect pulmonary vascular alterations indicating development of PH, a frequent comorbidity of COPD [2]. Previous investigations on the impact of ECV on global heart function could not find any ECV-induced alterations after short-term (14 days) [52] and long-term (8 months) [11] exposure in mice. However, 8 months of ECV exposure induced increased aortic stiffness [52]. Moreover, a recent study using high doses of nicotine induced PH development [53]. Thus, despite ECVE affecting PASMC *in vitro*, ECV *in vivo* did not induce pulmonary vascular remodelling in our setting.

A study limitation is the relatively low n-number in the *in vivo* experiments and the isolated lung setup, which may mask subtle changes in the different parameters assessed – especially regarding possible differences between NF ECV and ECV. However, the finding of the pronounced effect of ECV in these two independent experimental setups supports the conclusion that nicotine promotes the deleterious effects of e-cigarette vapour.

In summary, we showed that the presence of nicotine in e-cigarette vapour promoted acute endothelial damage, pulmonary inflammation and chronic pulmonary functional and structural alterations. Although research on e-cigarette use is hampered by the lack of standardisation in methods to produce and apply e-cigarette vapour, this diversity may reflect the variety of human situations in which application depends on e-liquid composition, puffing topography and e-cigarette characteristics [50].

Acknowledgment: The authors thank Christine Veith, Nils Schupp, Ingrid Breitenborn-Müller, Carmen Homberger, Elisabeth Kappes, Miriam Wessendorf, Susanne Lich, Christina Vroom and Karin Quanz for technical assistance.

Authors contributions: ETR, OP, RPB, NW and NS contributed to study design, data analysis, and interpretation; ETR, OP, AP, CGC, MB, DS, BS, DS, JS, KS, SK, SH, MG, DK, EMZ, BK, SH, IS, JW, JD and MH were study investigators who collected and assessed the data; ETR, OP NW, RPB and NS drafted the manuscript; MMAK, AT, FG, RTS, HAG, RPB and WS critically reviewed the manuscript. All authors reviewed and approved the final manuscript. E.T.R is designated the first co-author, as she performed all in vitro experiments and completed the project; O.P. is designated the second co-author, as he performed the in vivo experiments.

Conflict of interest: None declared

Support statement: This work was supported by the German Research Foundation (DFG) – Project-ID 268555672 – SFB 1213, A07 and CP02, and the Balzan prize to the research group of the German Center for Lung Research (DZL) – Erika von Mutius, Klaus F. Rabe, Werner Seeger and Tobias Welte.

a) Lung airways and parenchyma			
	Control vs. NF ECV	**Control vs. ECV**	**NF ECV vs. ECV**
Static compliance	Compatible	Compatible	Compatible
Resistance	Compatible	Compatible	Compatible
Inspiratory capacity	Compatible	Compatible	Compatible
Air/tissue, lung density*	Compatible	Compatible	Compatible
Airspace	Compatible	Compatible	Compatible
MLI	Compatible	Compatible	Compatible
n-number of compatible changes	**6**	**6**	**6**
Total n-number of analysed parameters	**6**	**6**	**6**
p-value	**0.031**	**0.031**	**0.031**

b) Pulmonary vasculature			
	Control vs. NF ECV	**Control vs. ECV**	**NF ECV vs. ECV**
Heart ratio	No change	Not compatible	Not compatible
RVSP	Compatible	Not Compatible	Compatible
RVWT	Compatible	Compatible	Compatible
TAPSE	Not compatible	Not compatible	Not compatible
Degree of muscularization	Not compatible	Not compatible	Not compatible
n-number of compatible changes	**2**	**1**	**2**
Total n-number of analysed parameters	**5**	**5**	**5**
p-value	**>0.99**	**>0.99**	**>0.99**

Table 1. Binominal analysis of parameters characterising a) lung airways and parenchyma, and b) the pulmonary vasculature. Binominal analysis of parameters characterising **a**) lung airways and parenchyma, and b) the pulmonary vasculature. „Compatible“ indicates that the parameter was compatible with a certain pathology

(smoke-induced emphysema or pulmonary hypertension) - marked in green colour; „Not compatible“ indicates that the parameter was not compatible with a certain pathology - marked in red colour; “No changes” indicates that the parameter was not changed - marked in blue colour. *dependent parameters, regarded as one variable. NF ECV: nicotine free e-cigarette vapour, ECV: nicotine-containing e-cigarette vapour, MLI: mean linear intercept, RVSP: right ventricular systolic pressure, RVWT: right ventricular weight, TAPSE: tricuspid annular plane systolic excursion. Binominal analysis was performed by using Binom.Dist in Excel.

References:

1. Finks SW, Rumbak MJ, Self TH. Treating Hypertension in Chronic Obstructive Pulmonary Disease. *N Engl J Med* 2020: 382(4): 353-363.

2. Gredic M, Blanco I, Kovacs G, Helyes Z, Ferdinandy P, Olschewski H, Barbera JA, Weissmann N. Pulmonary hypertension in chronic obstructive pulmonary disease. *Br J Pharmacol* 2020.

3. Pappas RS. Toxic elements in tobacco and in cigarette smoke: inflammation and sensitization. *Metallomics* 2011: 3(11): 1181-1198.

4. Huang J, Duan Z, Kwok J, Binns S, Vera LE, Kim Y, Szczypka G, Emery SL. Vaping versus JUULing: how the extraordinary growth and marketing of JUUL transformed the US retail e-cigarette market. *Tob Control* 2019: 28(2): 146-151.

5. Kaur G, Pinkston R, McLemore B, Dorsey WC, Batra S. Immunological and toxicological risk assessment of e-cigarettes. *Eur Respir Rev* 2018: 27(147).

6. Vardavas CI, Anagnostopoulos N, Kougias M, Evangelopoulou V, Connolly GN, Behrakis PK. Short-term pulmonary effects of using an electronic cigarette: impact on respiratory flow resistance, impedance, and exhaled nitric oxide. *Chest* 2012: 141(6): 1400-1406.

7. Schober W, Szendrei K, Matzen W, Osiander-Fuchs H, Heitmann D, Schettgen T, Jorres RA, Fromme H. Use of electronic cigarettes (e-cigarettes) impairs indoor air quality and increases FeNO levels of e-cigarette consumers. *Int J Hyg Environ Health* 2014: 217(6): 628-637.

8. Flouris AD, Chorti MS, Poulianiti KP, Jamurtas AZ, Kostikas K, Tzatzarakis MN, Wallace Hayes A, Tsatsakis AM, Koutedakis Y. Acute impact of active and passive electronic cigarette smoking on serum cotinine and lung function. *Inhal Toxicol* 2013: 25(2): 91-101.

9. Cherian SV, Kumar A, Estrada YMRM. E-cigarette or Vaping- product associated lung injury: A review. *Am J Med* 2020.

10. Garcia-Arcos I, Geraghty P, Baumlin N, Campos M, Dabo AJ, Jundi B, Cummins N, Eden E, Grosche A, Salathe M, Foronjy R. Chronic electronic cigarette exposure in mice induces features of COPD in a nicotine-dependent manner. *Thorax* 2016: 71(12): 1119-1129.

11. Olfert IM, DeVallance E, Hoskinson H, Branyan KW, Clayton S, Pitzer CR, Sullivan DP, Breit MJ, Wu Z, Klinkhachorn P, Mandler WK, Erdreich BH, Ducatman BS, Bryner RW, Dasgupta P, Chantler PD. Chronic exposure to electronic cigarettes results in impaired cardiovascular function in mice. *J Appl Physiol (1985)* 2018: 124(3): 573-582.

12. Bahl V, Lin S, Xu N, Davis B, Wang YH, Talbot P. Comparison of electronic cigarette refill fluid cytotoxicity using embryonic and adult models. *Reprod Toxicol* 2012: 34(4): 529-537.

13. Romagna G, Allifranchini E, Bocchietto E, Todeschi S, Esposito M, Farsalinos KE. Cytotoxicity evaluation of electronic cigarette vapor extract on cultured mammalian fibroblasts (ClearStream-LIFE): comparison with tobacco cigarette smoke extract. *Inhal Toxicol* 2013: 25(6): 354-361.

14. Misra M, Leverette RD, Cooper BT, Bennett MB, Brown SE. Comparative in vitro toxicity profile of electronic and tobacco cigarettes, smokeless tobacco and nicotine replacement therapy products: e-liquids, extracts and collected aerosols. *Int J Environ Res Public Health* 2014: 11(11): 11325-11347.

15. Rowell TR, Reeber SL, Lee SL, Harris RA, Nethery RC, Herring AH, Glish GL, Tarran R. Flavored e-cigarette liquids reduce proliferation and viability in the CALU3 airway epithelial cell line. *Am J Physiol Lung Cell Mol Physiol* 2017: 313(1): L52-L66.

16. Leslie LJ, Vasanthi Bathrinarayanan P, Jackson P, Mabiala Ma Muanda JA, Pallett R, Stillman CJP, Marshall LJ. A comparative study of electronic cigarette vapor extracts on airway-related cell lines in vitro. *Inhal Toxicol* 2017: 29(3): 126-136.

17. Seimetz M, Sommer N, Bednorz M, Pak O, Veith C, Hadzic S, Gredic M, Parajuli N, Kojonazarov B, Kraut S, Wilhelm J, Knoepp F, Henneke I, Pichl A, Kanbagli ZI, Scheibe S, Fysikopoulos A, Wu CY, Klepetko W, Jaksch P, Eichstaedt C, Grunig E, Hinderhofer K, Geiszt M, Muller N, Rezende F, Buchmann G, Wittig I, Hecker M, Hecker A, Padberg W, Dorfmuller P, Gattenlohner S, Vogelmeier CF, Gunther A, Karnati S, Baumgart-Vogt E, Schermuly RT, Ghofrani HA, Seeger W, Schroder K, Grimminger F, Brandes RP, Weissmann N. NADPH oxidase subunit NOXO1 is a target for emphysema treatment in COPD. *Nat Metab* 2020: 2(6): 532-546.

18. Sommer N, Huttemann M, Pak O, Scheibe S, Knoepp F, Sinkler C, Malczyk M, Gierhardt M, Esfandiary A, Kraut S, Jonas F, Veith C, Aras S, Sydykov A, Alebrahimdehkordi N, Giehl K, Hecker M, Brandes RP, Seeger W, Grimminger F, Ghofrani HA, Schermuly RT, Grossman LI, Weissmann N. Mitochondrial Complex IV Subunit 4 Isoform 2 Is Essential for Acute Pulmonary Oxygen Sensing. *Circ Res* 2017: 121(4): 424-438.

19. Seeger W, Walmrath D, Menger M, Neuhof H. Increased lung vascular permeability after arachidonic acid and hydrostatic challenge. *J Appl Physiol (1985)* 1986: 61(5): 1781-1789.

20. Kojonazarov B, Hadzic S, Ghofrani HA, Grimminger F, Seeger W, Weissmann N, Schermuly RT. Severe Emphysema in the SU5416/Hypoxia Rat Model of Pulmonary Hypertension. *Am J Respir Crit Care Med* 2019: 200(4): 515-518.

21. Peteranderl C, Morales-Nebreda L, Selvakumar B, Lecuona E, Vadasz I, Morty RE, Schmoldt C, Bespalowa J, Wolff T, Pleschka S, Mayer K, Gattenloehner S, Fink L, Lohmeyer J, Seeger W, Sznajder JI, Mutlu GM, Budinger GR, Herold S.

Macrophage-epithelial paracrine crosstalk inhibits lung edema clearance during influenza infection. *J Clin Invest* 2016: 126(4): 1566-1580.

22. Herold S, Tabar TS, Janssen H, Hoegner K, Cabanski M, Lewe-Schlosser P, Albrecht J, Driever F, Vadasz I, Seeger W, Steinmueller M, Lohmeyer J. Exudate macrophages attenuate lung injury by the release of IL-1 receptor antagonist in gram-negative pneumonia. *Am J Respir Crit Care Med* 2011: 183(10): 1380-1390.

23. Gredic M, Wu CY, Hadzic S, Pak O, Savai R, Kojonazarov B, Doswada S, Weiss A, Weigert A, Guenther A, Brandes RP, Schermuly RT, Grimminger F, Seeger W, Sommer N, Kraut S, Weissmann N. Myeloid-cell-specific deletion of inducible nitric oxide synthase protects against smoke-induced pulmonary hypertension in mice. *Eur Respir J* 2022: 59(4).

24. Seimetz M, Parajuli N, Pichl A, Veit F, Kwapiszewska G, Weisel FC, Milger K, Egemnazarov B, Turowska A, Fuchs B, Nikam S, Roth M, Sydykov A, Medebach T, Klepetko W, Jaksch P, Dumitrascu R, Garn H, Voswinckel R, Kostin S, Seeger W, Schermuly RT, Grimminger F, Ghofrani HA, Weissmann N. Inducible NOS inhibition reverses tobacco-smoke-induced emphysema and pulmonary hypertension in mice. *Cell* 2011: 147(2): 293-305.

25. Huang J, Yang G, Xiong X, Wang M, Yuan J, Zhang Q, Gong C, Qiu Z, Meng Z, Xu R, Chen Q, Chen R, Xie L, Xie Q, Zi W, Jiang G, Zhou Y, Yang Q. Age-related CCL12 Aggravates Intracerebral Hemorrhage-induced Brain Injury via Recruitment of Macrophages and T Lymphocytes. *Aging Dis* 2020: 11(5): 1103-1115.

26. Jia GQ, Gonzalo JA, Lloyd C, Kremer L, Lu L, Martinez AC, Wershil BK, Gutierrez-Ramos JC. Distinct expression and function of the novel mouse chemokine monocyte chemotactic protein-5 in lung allergic inflammation. *J Exp Med* 1996: 184(5): 1939-1951.

27. Yang P, Chen W, Xu H, Yang J, Jiang J, Jiang Y, Xu G. Correlation of CCL8 expression with immune cell infiltration of skin cutaneous melanoma: potential as a prognostic indicator and therapeutic pathway. *Cancer Cell Int* 2021: 21(1): 635.

28. Mukherjee M, Nair P. Autoimmune Responses in Severe Asthma. *Allergy Asthma Immunol Res* 2018: 10(5): 428-447.

29. Ross SH, Cantrell DA. Signaling and Function of Interleukin-2 in T Lymphocytes. *Annu Rev Immunol* 2018: 36: 411-433.

30. Blattman JN, Grayson JM, Wherry EJ, Kaech SM, Smith KA, Ahmed R. Therapeutic use of IL-2 to enhance antiviral T-cell responses in vivo. *Nat Med* 2003: 9(5): 540-547.

31. Miller AM. Role of IL-33 in inflammation and disease. *J Inflamm (Lond)* 2011: 8(1): 22.

32. E-Cigarette Use Among Youth and Young Adults: A Report of the Surgeon General, Atlanta (GA), 2016.

33. Dalle-Donne I, Garavaglia ML, Colombo G, Astori E, Lionetti MC, La Porta CAM, Santucci A, Rossi R, Giustarini D, Milzani A. Cigarette smoke and glutathione: Focus on in vitro cell models. *Toxicol In Vitro* 2020: 65: 104818.

34. Bazzini C, Rossetti V, Civello DA, Sassone F, Vezzoli V, Persani L, Tiberio L, Lanata L, Bagnasco M, Paulmichl M, Meyer G, Garavaglia ML. Short- and long- term effects of cigarette smoke exposure on glutathione homeostasis in human bronchial epithelial cells. *Cell Physiol Biochem* 2013: 32(7): 129-145.

35. Zhao J, Zhang Y, Sisler JD, Shaffer J, Leonard SS, Morris AM, Qian Y, Bello D, Demokritou P. Assessment of reactive oxygen species generated by electronic cigarettes using acellular and cellular approaches. *J Hazard Mater* 2018: 344: 549-557.

36. Lilly CM, Khan S, Waksmundzki-Silva K, Irwin RS. Vaping-Associated Respiratory Distress Syndrome: Case Classification and Clinical Guidance. *Crit Care Explor* 2020: 2(2): e0081.

37. Diabasana Z, Perotin JM, Belgacemi R, Ancel J, Mulette P, Delepine G, Gosset P, Maskos U, Polette M, Deslee G, Dormoy V. Nicotinic Receptor Subunits Atlas in the Adult Human Lung. *Int J Mol Sci* 2020: 21(20).

38. Rounds S, Lu Q. Cigarette smoke alters lung vascular permeability and endothelial barrier function (2017 Grover Conference Series). *Pulm Circ* 2018: 8(3): 2045894018794000.

39. Christiani DC. Vaping-Induced Acute Lung Injury. *N Engl J Med* 2020: 382(10): 960-962.

40. Dupuy PM, Lancon JP, Francoise M, Frostell CG. Inhaled cigarette smoke selectively reverses human hypoxic vasoconstriction. *Intensive Care Med* 1995: 21(11): 941-944.

41. Horikawa K, Takatsu K. Interleukin-5 regulates genes involved in B-cell terminal maturation. *Immunology* 2006: 118(4): 497-508.

42. Gour N, Wills-Karp M. IL-4 and IL-13 signaling in allergic airway disease. *Cytokine* 2015: 75(1): 68-78.

43. Lerner CA, Sundar IK, Yao H, Gerloff J, Ossip DJ, McIntosh S, Robinson R, Rahman I. Vapors produced by electronic cigarettes and e-juices with flavorings induce toxicity, oxidative stress, and inflammatory response in lung epithelial cells and in mouse lung. *PLoS One* 2015: 10(2): e0116732.

44. Sussan TE, Gajghate S, Thimmulappa RK, Ma J, Kim JH, Sudini K, Consolini N, Cormier SA, Lomnicki S, Hasan F, Pekosz A, Biswal S. Exposure to electronic cigarettes impairs pulmonary anti-bacterial and anti-viral defenses in a mouse model. *PLoS One* 2015: 10(2): e0116861.

45. Song MA, Reisinger SA, Freudenheim JL, Brasky TM, Mathe EA, McElroy JP, Nickerson QA, Weng DY, Wewers MD, Shields PG. Effects of Electronic Cigarette Constituents on the Human Lung: A Pilot Clinical Trial. *Cancer Prev Res (Phila)* 2020: 13(2): 145-152.

46. Wells JM, Parker MM, Oster RA, Bowler RP, Dransfield MT, Bhatt SP, Cho MH, Kim V, Curtis JL, Martinez FJ, Paine R, 3rd, O'Neal W, Labaki WW, Kaner RJ, Barjaktarevic I, Han MK, Silverman EK, Crapo JD, Barr RG, Woodruff P, Castaldi PJ, Gaggar A, Spiromics, Investigators CO. Elevated circulating MMP-9 is linked to increased COPD exacerbation risk in SPIROMICS and COPDGene. *JCI Insight* 2018: 3(22).

47. Baggio C, Velazquez JV, Fragai M, Nordgren TM, Pellecchia M. Therapeutic Targeting of MMP-12 for the Treatment of Chronic Obstructive Pulmonary Disease. *J Med Chem* 2020: 63(21): 12911-12920.

48. Larcombe AN, Janka MA, Mullins BJ, Berry LJ, Bredin A, Franklin PJ. The effects of electronic cigarette aerosol exposure on inflammation and lung function in mice. *Am J Physiol Lung Cell Mol Physiol* 2017: 313(1): L67-L79.

49. Yingst JM, Foulds J, Veldheer S, Hrabovsky S, Trushin N, Eissenberg TT, Williams J, Richie JP, Nichols TT, Wilson SJ, Hobkirk AL. Nicotine absorption during electronic cigarette use among regular users. *PLoS One* 2019: 14(7): e0220300.

50. *In:* Eaton DL, Kwan LY, Stratton K, eds. Public Health Consequences of E-Cigarettes, Washington (DC), 2018.

51. Polosa R, Cibella F, Caponnetto P, Maglia M, Prosperini U, Russo C, Tashkin D. Health impact of E-cigarettes: a prospective 3.5-year study of regular daily users who have never smoked. *Sci Rep* 2017: 7(1): 13825.

52. Shi H, Fan X, Horton A, Haller ST, Kennedy DJ, Schiefer IT, Dworkin L, Cooper CJ, Tian J. The Effect of Electronic-Cigarette Vaping on Cardiac Function and Angiogenesis in Mice. *Sci Rep* 2019: 9(1): 4085.

53. Oakes JM, Xu J, Morris TM, Fried ND, Pearson CS, Lobell TD, Gilpin NW, Lazartigues E, Gardner JD, Yue X. Effects of Chronic Nicotine Inhalation on Systemic and Pulmonary Blood Pressure and Right Ventricular Remodeling in Mice. *Hypertension* 2020: 75(5): 1305-1314.

Figures

Figure 1. Effect of *in vitro* ECVE or NF ECVE exposure on metabolic activity and proliferation

a, b) Cell metabolic activity of primary mouse ATII cells (mATII, **a**, n=6), and primary mouse PASMC (mPASMC, **b**, n=5) after exposure to different concentrations of either nicotine-free e-cigarette vapour extract (NF ECVE), nicotine-containing e-cigarette vapour extract (ECVE) or conventional cigarette smoke extract (CSE). Data are presented as percent of control. **c)** Cell proliferation of mPASMC (n=8) after exposure to either 15% NF ECVE, 15% ECVE, 5% CSE or control. Data are presented as percent of control. **d, e)** Cell metabolic activity of primary human bronchial epithelial cells (HBEpC, **d**, n=6) and primary human PASMC (hPASMC, **e**, n=5) after exposure to different concentrations of either NF ECVE, ECVE or conventional CSE. Data are presented as percent of control. **f)** Cell proliferation of hPASMC (n=6) after exposure to either 15% NF ECVE, 15% ECVE, 5% CSE or control. Data are presented as percent of control. Controls were treated with medium without ECVE, NF ECVE or CSE. n of mATII cells, mPASMC and hPASMC represents independent isolations per group, n of HBEpC represents independent experiments per group. Statistical analysis was performed by one-way ANOVA with Tukeys post hoc-test. Significant p-values in comparison to respective controls are presented. Data are presented as mean ± SEM.

Figure 2. The effects of ECVE or NF ECV on gene expression patterns, glutathione levels and protein expression of the autophagy-lysosome system.

a, b) Gene ontology (GO) enrichment analysis of differentially expressed mRNA transcripts in primary mATII cells (**a**) and primary mPASMC (**b**) exposed to either 15% nicotine-free e-cigarette vapour extract (NF ECVE) or 15% nicotine-containing e-

cigarette vapour extract (ECVE). Bubble plots for enrichment analysis of GO terms are presented. The bubble areas indicate the number of genes in the sets, and the colour indicates if most of GO terms were up- (red), or downregulated (green). Yellow colour indicates that both up- and downregulated genes contribute to the enrichment. n=8. The y-axis [-log(p)] displays the significance level, the x-axis the percentage of expressed genes in the respective set of genes for a specific pathway. **c)** Level of the GSH/GSSG ratio in primary mATII cells exposed to either 15% NF ECVE, 15% ECVE, 2.5% CSE or control medium without ECVE, NF ECVE or CSE. n=8 each. **d)** Protein expression of p62 and LC3-II, normalised to the expression of β-actin in primary mPASMC exposed to either 15% NF ECVE, 15% ECVE or control medium without ECVE or NF ECVE. n=4. n-numbers represent independent isolations per group. For statistical analysis of c,d one-way ANOVA with Tukeys post hoc-test was used. Data are presented as mean ± SEM.

Figure 3. ECV inhalation increased endothelial permeability in isolated perfused and ventilated mouse lungs.

a) Effect of nicotine-free e-cigarette vapour (NF ECV) or nicotine-containing e-cigarette vapour (ECV) on hypoxic pulmonary vasoconstriction (HPV). **b)** Effect of NF ECV or ECV on the capillary filtration coefficient (K_{fc}). HPV was determined as the maximum increase of pulmonary arterial pressure (ΔPAP) during hypoxic ventilation. K_{fc} was measured gravimetrically and calculated from the slope of lung weight gain induced by an increase of the pulmonary venous pressure from 2 to 10mmHg. Data are provided as percent change of ΔPAP and K_{fc} compared to the reference hypoxic manoeuvre or pressure challenge without NF ECV or ECV. n=5-6 isolated mouse lungs per group, control lungs were ventilated without NF ECV or ECV. Statistical analysis was

performed by one-way ANOVA with Tukeys post hoc-test. Data are presented as mean ± SEM.

Figure 4. Effect of long-term *in vivo* exposure to ECV or NF ECV on pulmonary inflammation.

a-d) Total number of cells (**a**), neutrophils (**b**), lymphocytes (**c**) and macrophages (**d**) in bronchoalveolar lavage (BAL) from mice exposed to nicotine-free e-cigarette vapour (NF ECV) or nicotine-containing e-cigarette vapour (ECV) for 8 months. **e, f)** Number of macrophages given for exudate macrophages (ExMAs, **e**) and residence macrophages (rAM, **f**). Values are given as percentage of total macrophages. a-f) n=5 mice per group. **g)** Levels of selected inflammatory mediators in the bronchoalveolar lavage fluid (BALF=BAL supernatant) from mice exposed to NF ECV or ECV for 8 months (n=10 mice per group). **h)** Number of CD45+ cells located around vessels, alveolar septa or bronchi in lung sections of mice exposed to NF ECV or ECV for 8 months according to the following scale: 0 – little number of CD45+ cells, 1 – moderate number of CD45+ cells, and 2 – many CD45+ cells (n=6 lungs per group). **i)** Number of CD3+ cells per lung section area in mice exposed to NF ECV or ECV for 8 months (n=5 lungs per group). **j)** Representative images of lung sections from mice exposed to NF ECV or ECV stained for CD3+ and CD45+ cells. Control animals (Ctrl) received room air only. Statistical analysis: (a-g, i) one-way ANOVA with Tukeys post hoc-test. (h) Categorical analysis was done using pair-wise Wilcoxon-tests with continuity correction. Data are presented as mean ± SEM.

Figure 5. Effect of long-term *in vivo* exposure to ECV or NF ECV on lung functional and structural parameters in mice.

a-d) Lung functional parameters (n=9-11), static compliance (**a**), resistance (**b**), inspiratory capacity (**c**), pressure-volume loops (**d**) of mice exposed to nicotine-free e-cigarette vapour (NF ECV), nicotine-containing e-cigarette vapour (ECV) or room air (control, ctrl) for 8 months. **e-j)** Lung structural parameters from *in vivo* µCT measurements (n=9-12), air/tissue ratio (**e**), lung density (**f**), representative µCT imaging (**g**) or histological analysis (n=6), airspace (**h**), mean linear intercept (**i**), representative pictures (**j**). Lung sections were stained with haematoxylin and eosin (scale bars 250µm). Statistical analysis: one-way ANOVA with Tukeys post hoc-test. Combined p-value from e, f, g): p=0.03 determined by meta-analysis according to the Fisher's method using 'BisRNA' R package. Data are presented as mean ± SEM.

Figure 6. Effect of long-term *in vivo* exposure to ECV or NF ECV on the pulmonary circulation in mice.

a, b) Hemodynamic measurements (n=9-12), right ventricular systolic pressure (RVSP, **a**) and systolic arterial pressure (SAP, **b**). **c)** Morphological analysis of pulmonary vessels. Data are given as percentage of fully, partially or not muscularised vessels of total vessel count (n=6). **d)** Heart ratio (ratio of the weight of the right ventricle (RV) and the left ventricle plus septum (LV+S)), n=10-11. The LV+S weight was not changed between the groups. **e-h)** Echocardiographic analysis of right ventricular wall thickness (RVWT, **e**), tricuspid annular plane systolic excursion (TAPSE, **f**) and cardiac index (**g**) (n=4-7 each); representative images of echocardiography (**h**). Data were assessed from mice either exposed to nicotine-free e-cigarette vapour (NF ECV), nicotine-containing e-cigarette vapour (ECV) or room air (Control, Ctrl) for 8 months. Statistical analysis was performed by one-way ANOVA with Tukeys post hoc-test. Data are presented as mean ± SEM.

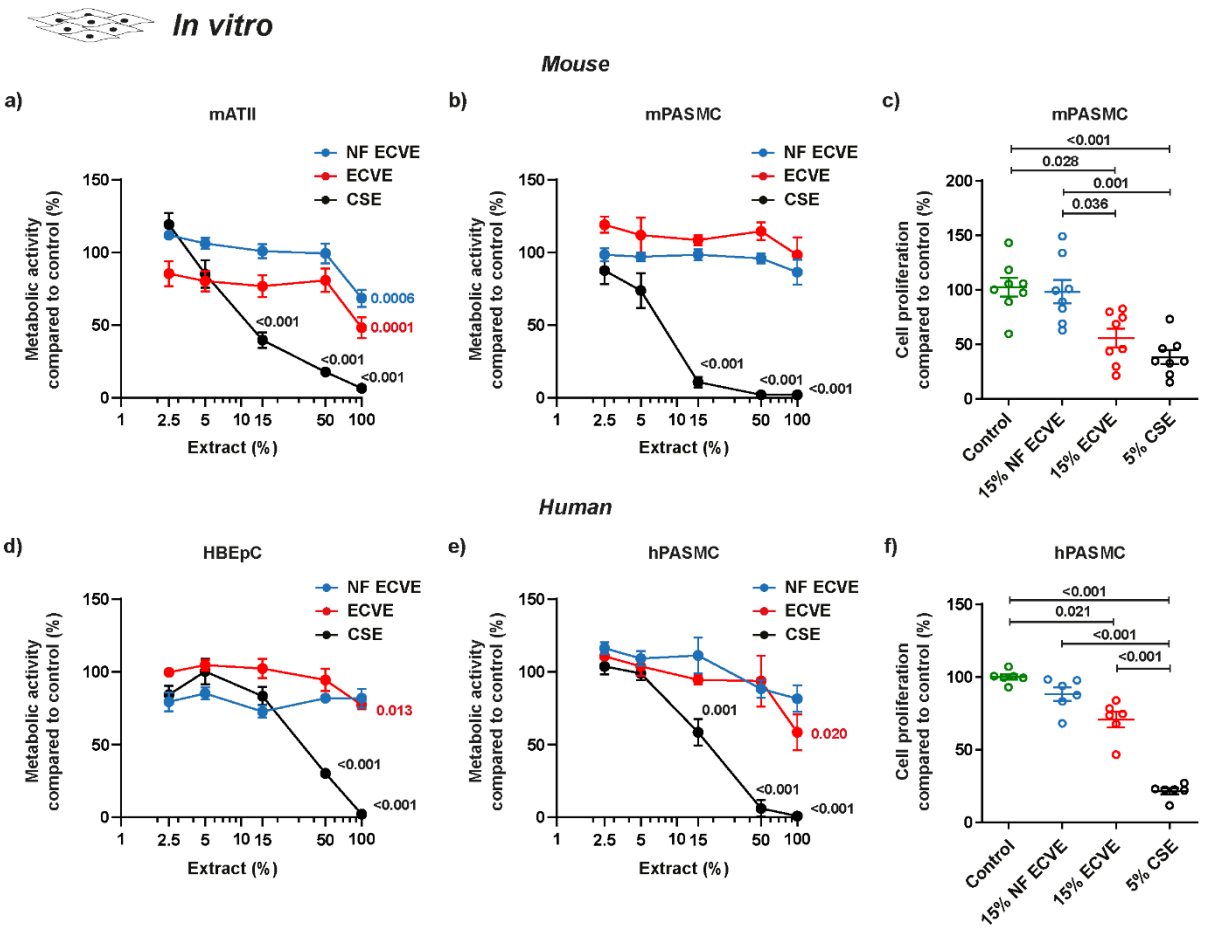
In vitro
Mouse
a)
mATII
NF ECVE
ECVE
CSE
Metabolic activity compared to control (%)
Extract (%)
0.0006
0.0001
<0.001
<0.001
<0.001
b)
mPASMC
NF ECVE
ECVE
CSE
Metabolic activity compared to control (%)
Extract (%)
<0.001
<0.001
<0.001
c)
mPASMC
Cell proliferation compared to control (%)
<0.001
0.028
0.001
0.036
Control
15% NF ECVE
15% ECVE
5% CSE
Human
d)
HBEpC
NF ECVE
ECVE
CSE
Metabolic activity compared to control (%)
Extract (%)
0.013
<0.001
<0.001
e)
hPASMC
NF ECVE
ECVE
CSE
Metabolic activity compared to control (%)
Extract (%)
0.001
0.020
<0.001
<0.001
f)
hPASMC
Cell proliferation compared to control (%)
<0.001
0.021
<0.001
<0.001
Control
15% NF ECVE
15% ECVE
5% CSE

Figure 1

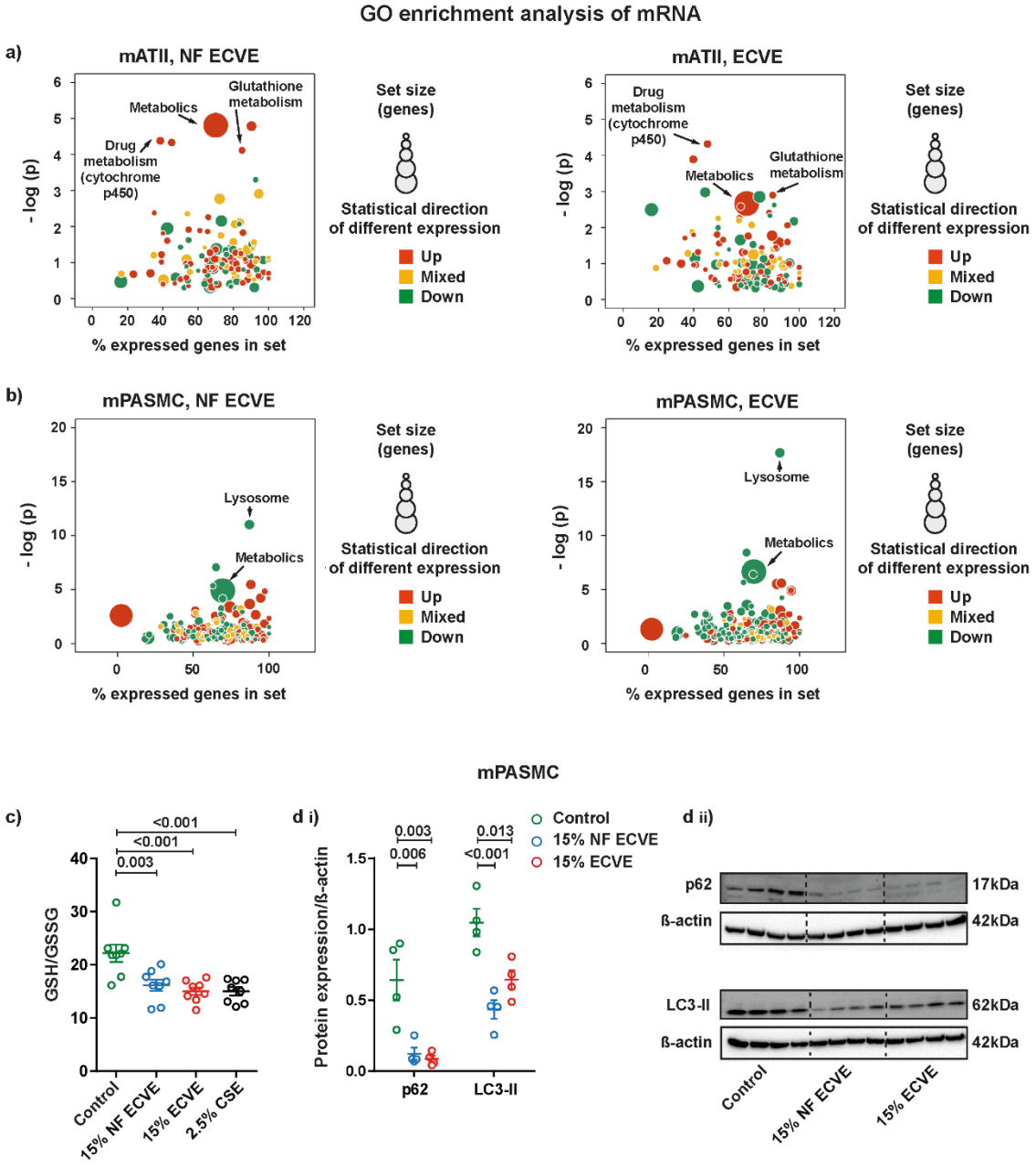
GO enrichment analysis of mRNA
a)
mATII, NF ECVE
Metabolics
Glutathione metabolism
Drug metabolism (cytochrome p450)
- log (p)
% expressed genes in set
Set size (genes)
Statistical direction of different expression
Up
Mixed
Down
mATII, ECVE
Drug metabolism (cytochrome p450)
Metabolics
Glutathione metabolism
b)
mPASMC, NF ECVE
Lysosome
Metabolics
mPASMC, ECVE
mPASMC
c)
GSH/GSSG
<0.001
<0.001
0.003
Control
15% NF ECVE
15% ECVE
2.5% CSE
d i)
Protein expression/ß-actin
0.003
0.006
0.013
<0.001
p62
LC3-II
Control
15% NF ECVE
15% ECVE
d ii)
p62
17kDa
ß-actin
42kDa
LC3-II
62kDa
ß-actin
42kDa
Control
15% NF ECVE
15% ECVE

Figure 2

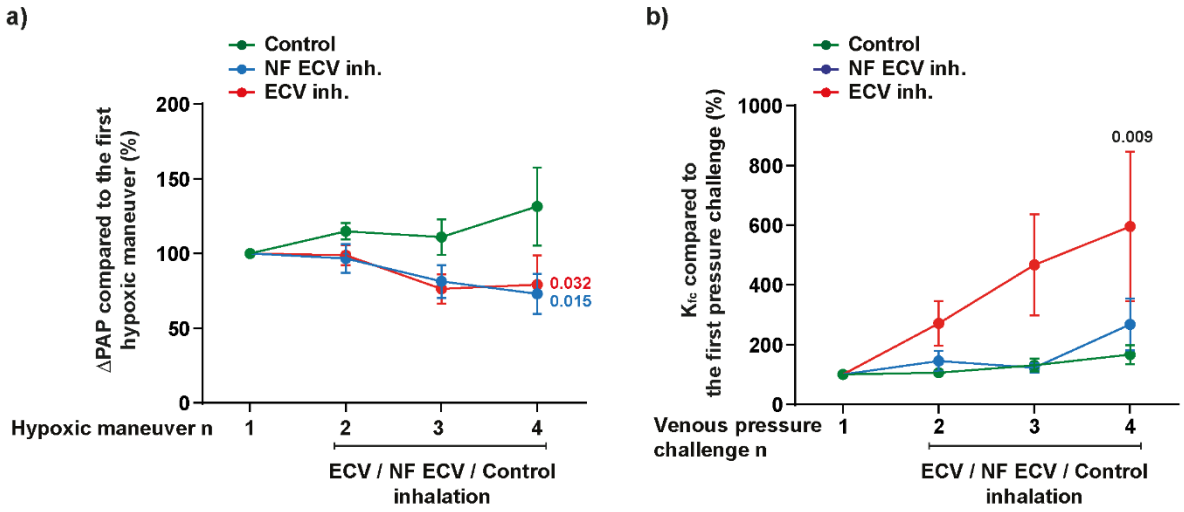
a)
Control
NF ECV inh.
ECV inh.
ΔPAP compared to the first hypoxic maneuver (%)
200
150
100
50
0
0.032
0.015
Hypoxic maneuver n
1
2
3
4
ECV / NF ECV / Control inhalation
b)
Control
NF ECV inh.
ECV inh.
Kfc compared to the first pressure challenge (%)
1000
800
600
400
200
0
0.009
Venous pressure challenge n
1
2
3
4
ECV / NF ECV / Control inhalation

Figure 3

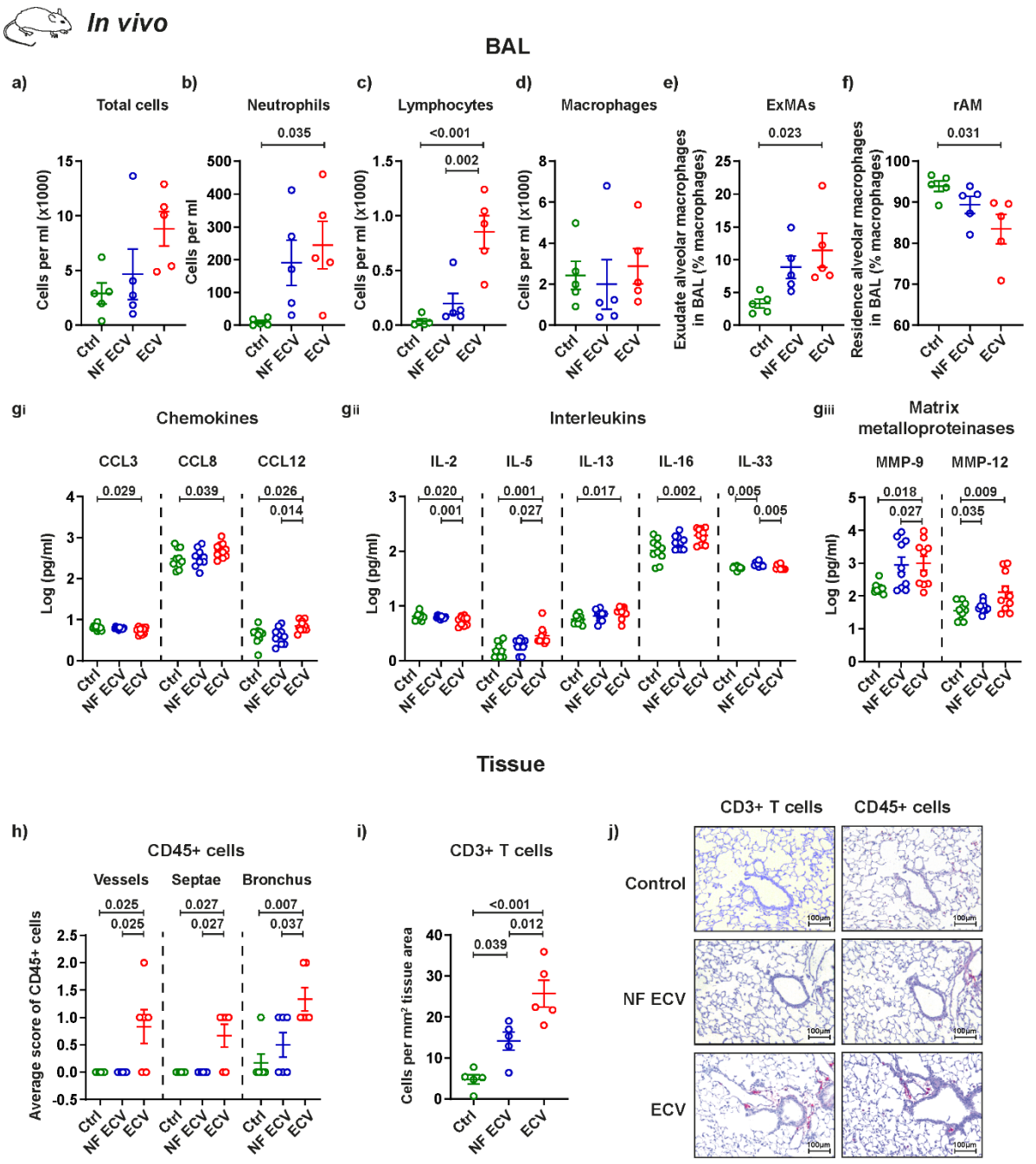
In vivo
BAL
a)
Total cells
Cells per ml (x1000)
b)
Neutrophils
Cells per ml
0.035
c)
Lymphocytes
Cells per ml (x1000)
<0.001
0.002
d)
Macrophages
Cells per ml (x1000)
e)
ExMAs
Exudate alveolar macrophages in BAL (% macrophages)
0.023
f)
rAM
Residence alveolar macrophages in BAL (% macrophages)
0.031
Ctrl
NF ECV
ECV
gi
Chemokines
CCL3
CCL8
CCL12
Log (pg/ml)
0.029
0.039
0.026
0.014
gii
Interleukins
IL-2
IL-5
IL-13
IL-16
IL-33
0.020
0.001
0.027
0.017
0.002
0.005
0.005
giii
Matrix metalloproteinases
MMP-9
MMP-12
0.018
0.027
0.009
0.035
Tissue
h)
CD45+ cells
Vessels
Septae
Bronchus
Average score of CD45+ cells
0.025
0.025
0.027
0.027
0.007
0.037
i)
CD3+ T cells
Cells per mm² tissue area
<0.001
0.012
0.039
j)
CD3+ T cells
CD45+ cells
Control
NF ECV
ECV
100µm

Figure 4

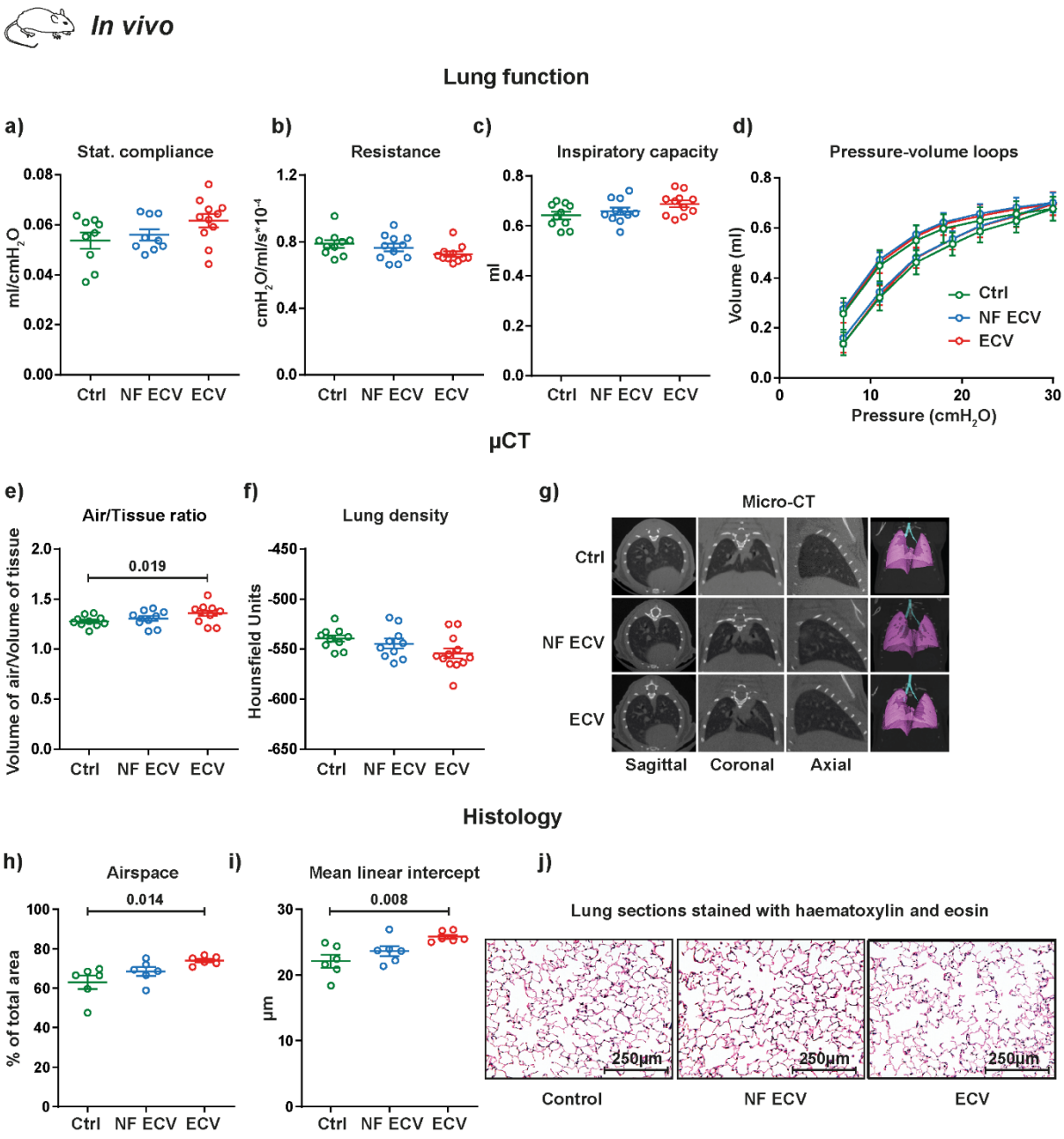
In vivo
Lung function
a)
Stat. compliance
ml/cmH2O
0.08
0.06
0.04
0.02
0.00
Ctrl NF ECV ECV
b)
Resistance
cmH2O/ml/s*10-4
1.2
0.8
0.4
0.0
Ctrl NF ECV ECV
c)
Inspiratory capacity
ml
0.8
0.6
0.4
0.2
0.0
Ctrl NF ECV ECV
d)
Pressure-volume loops
Volume (ml)
0.8
0.6
0.4
0.2
0.0
0 10 20 30
Pressure (cmH2O)
Ctrl
NF ECV
ECV
µCT
e)
Air/Tissue ratio
Volume of air/Volume of tissue
2.0
1.5
1.0
0.5
0.0
0.019
Ctrl NF ECV ECV
f)
Lung density
Hounsfield Units
-450
-500
-550
-600
-650
Ctrl NF ECV ECV
g)
Micro-CT
Ctrl
NF ECV
ECV
Sagittal Coronal Axial
Histology
h)
Airspace
% of total area
100
80
60
40
20
0
0.014
Ctrl NF ECV ECV
i)
Mean linear intercept
µm
30
20
10
0
0.008
Ctrl NF ECV ECV
j)
Lung sections stained with haematoxylin and eosin
250µm
250µm
250µm
Control
NF ECV
ECV

Figure 5

In vivo

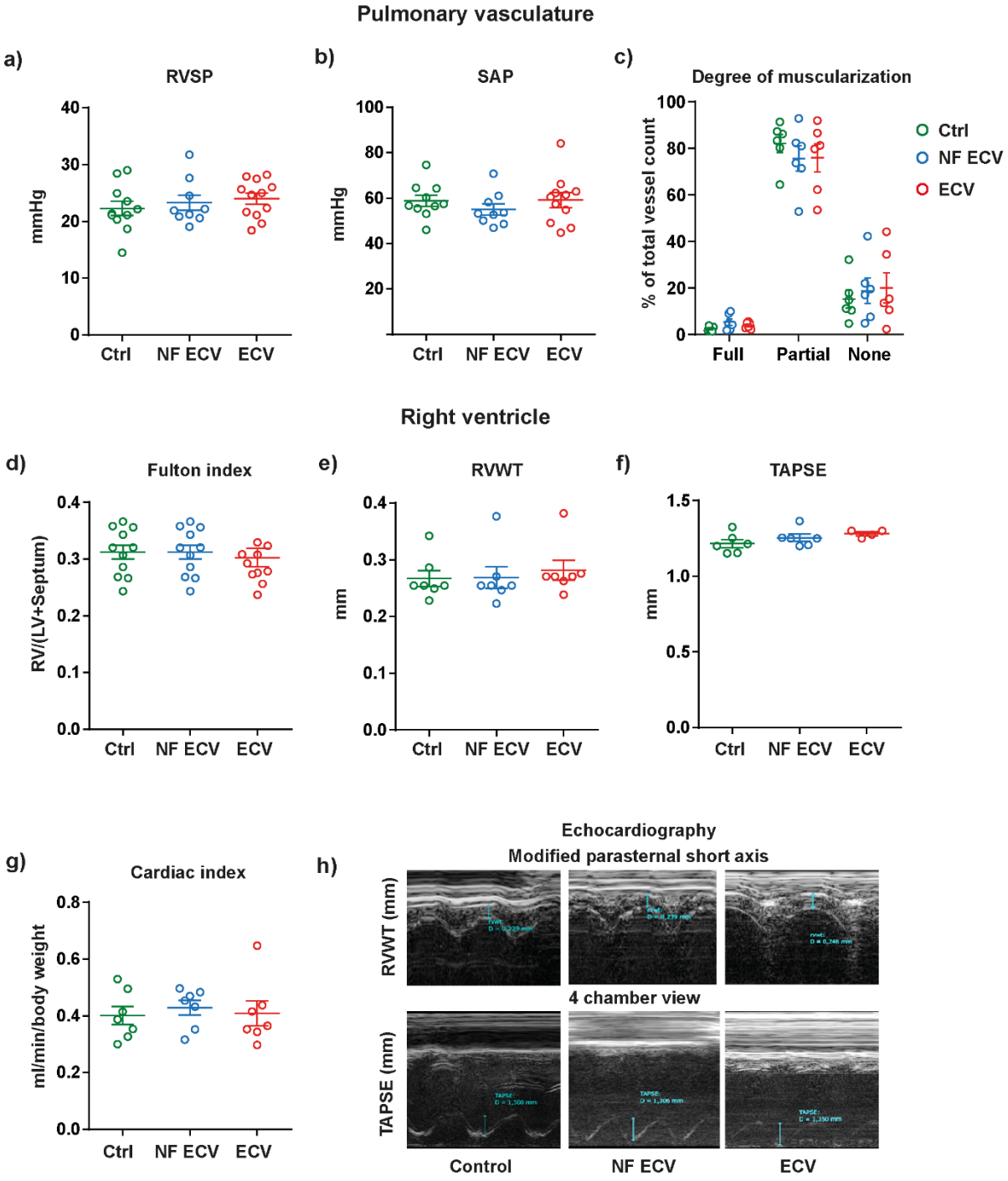

Figure 6

SUPPLEMENTARY MATERIAL

Nicotine promotes e-cigarette vapour-induced lung inflammation and structural alterations

Elsa T. Roxlau, Oleg Pak, Stefan Hadzic, Claudia F. Garcia-Castro, Marija Gredic, Cheng-Yu Wu, Julia Schäffer, Balachandar Selvakumar, Alexandra Pichl, David Spiegelberg, Janik Deutscher, Mariola Bednorz, Katharina Schäfer, Simone Kraut, Djuro Kosanovic, Esraa M Zeidan, Baktybek Kojonazarov, Susanne Herold, Ievgen Strielkov, Andreas Guenther, Jochen Wilhelm, Mohamed M. A. Khalifa, Ashraf Taye, Ralf P. Brandes, Matthias Hecker, Friedrich Grimminger, Hossein A. Ghofrani, Ralph T. Schermuly, Werner Seeger, Natascha Sommer, Norbert Weissmann.

SUPPLEMENTARY METHODS

Cell culture

All cells were cultured in a humidified atmosphere of 5% CO_2 at 37°C in a cell incubator and used 24 h after seeding. For the 3-(4,5-dimethylthiazol-2-yl)-2,5-diphenyl-2H-tetrazolium bromide (MTT), lactate dehydrogenase activity (LDH, cytotoxic assay) and apoptosis assay, cells were seeded in 96-well plates in the following concentrations: 10,000 cells/well for A549, human pulmonary arterial smooth muscle cells (hPASMC), and primary mouse pulmonary arterial smooth muscle cells (mPASMC), 20,000 cells/well for human bronchial epithelial cells (HBEpC), and 140,000 cells/well for mouse alveolar epithelial type II cells (mATII) cells. For analyses of cell confluence and the number of dead cells (BOBO™-3 iodide staining), mPASMC and hPASMC cells were seeded in 96-well plates (both cell types 10,000 cells/well), for the BrdU

proliferation assay in 24-well plates (both cell types 20,000 cells/well), for the migration assay in 2-well Ibidi culture-inserts (Ibidi GmbH, Gräfelfing, Germany) (2,500 cells/well of hPASMC and 5,000 cells/well of mPASMC), and for the real-time PCR, Western blot and microarray in 6-well plates (both cell types 60,000 cells/well). 140,000 cells/well and 3,000,000 cells/well of mATII were seeded in 96-well plates and 6-well plates for the glutathione assay and real-time PCR/microarray, respectively. The following media were used in the study: DMEM (Thermo Fisher Scientific, Waltham, USA) with 10% FCS (Sigma-Aldrich, Burlington, USA) for A549 and mATII cells, airway epithelial cell growth medium (PromoCell, Heidelberg, Germany) with 10% FCS for HBEpC, smooth muscle cell growth medium (PromoCell, Heidelberg, Germany) with supplement and 10% FCS for mPASMC and without FCS for hPASMC.

Isolation of primary mouse pulmonary arterial smooth muscle cells (mPASMC)

mPASMC were isolated from precapillary pulmonary arterial vessels as described previously [1]. Briefly, 3ml of M199 (Medium 199, Invitrogen, Carlsbad, USA) containing 5mg/ml low melting point agarose, 5mg/ml Fe_3O_4 (Sigma-Aldrich, Burlington, USA), and 1% penicillin/streptomycin was injected into the pulmonary artery and the lung was fixated via agarose injection into the trachea. Subsequently, the lung was cut with scissors for 5 min into tiny pieces, which were maintained in 10ml PBS. The pieces from the pulmonary arterial vessels containing Fe_3O_4 (Sigma-Aldrich, Burlington, USA) were collected using a magnet in a magnetic holder and digested in 10ml of M199, containing 80U/ml collagenase (Sigma-Aldrich, Burlington, USA) at 37°C for 60 min. The tissue mixture was disrupted by passing it through 15 and 18-gauge needles 5–6 times each. The resulting suspension, containing the medial and intimal layer of the pulmonary arterial vessels attached to Fe_3O_4 (Sigma-Aldrich, Burlington, USA) particles, was rinsed three times with M199 (Thermo Fisher Scientific,

Waltham, USA), containing 10% FCS, in the magnetic holder. These pieces were re-suspended in smooth muscle cell growth medium (PromoCell, Heidelberg, Germany) with a supplement and 10% FCS, transferred to culture flasks and incubated at 37°C in a cell incubator to induce outgrowth of smooth muscle cells. Upon reaching 80% confluence, the grown mPASMC were trypsinised and seeded into new culture flasks (=first passage). The experiments were performed with mPASMC in the second passage.

Isolation of primary human pulmonary artery smooth muscle cells (hPASMC)

The hPASMC were isolated from pulmonary arteries of donor lung transplants. The studies were approved by the ethics committee of the Justus-Liebig University (AZ 58/15, AZ 10/06). Briefly, pulmonary arteries were dissected from the lung transplant. Then, the medial layer was separated from the adventitial and endothelial layers under a microscope. The medial layer of the arteries was minced using scalpels, transferred to Petri dishes, and cultured with 10ml of smooth muscle cell growth medium (PromoCell, Heidelberg, Germany) containing a supplement (PromoCell, Heidelberg, Germany) to induce outgrowth of hPASMC.

Isolation of primary mouse alveolar epithelial type II cells (mATII)

The mATII cells were isolated from mouse lungs using a modification of the method described previously [2]. After perfusion of the lung through the pulmonary artery with 3ml of saline, 2ml of dispase (Corning, Corning, USA) was instilled intratracheally. The lungs were removed from the chest cavity, placed in a 50ml falcon tube containing 2ml of dispase and incubated for 30 min at 37°C. Then, the lungs were transferred to a 50ml falcon tube containing 2ml DMEM (Thermo Fisher Scientific, Waltham, USA), 0.04mg/ml DNase (Sigma-Aldrich, Burlington, USA) and 1ml FCS (Sigma-Aldrich,

Burlington, USA) to stop dispase activity. After a brief stirring, the lungs were transferred to a 100 mm culture dish. The heart, oesophagus and trachea were carefully removed, and the lung tissue was minced using two scissors. The cell suspension was filtered through a 70µm, 40µm and 10µm nylon mesh cell strainer and centrifuged at 200g for 10 min (15°C). After centrifugation, the supernatant was discarded, and the cell pellet was re-suspended with 1ml DMEM (Thermo Fisher Scientific, Waltham, USA). Crude cell suspensions were purified by the negative selection of immune cells using 100 mm tissue culture plates, coated with a mixture of 0.75µg/ml CD16/32 (#553142, BD Biosciences, Franklin Lakes, USA) and 0.75µg/ml CD45 (#553076, BD Biosciences, Franklin Lakes, USA). After incubation for 45 min at 37°C, the cell suspension was placed in uncoated 100 mm tissue culture plates and incubated for 45 min at 37°C. The cell suspension was collected in a 50ml falcon tube and centrifuged at 200g for 10min (15°C). Afterwards, the cell suspension was treated with 2ml of erythrocyte red blood cell lysing buffer (BD Biosciences, Franklin Lakes, USA) for 5 min. The reaction was stopped by adding 4ml of DMEM. The suspension was centrifuged at 200g for 10 min (15°C). The mATII were re-suspended in DMEM medium (Thermo Fisher Scientific, Waltham, USA) plus 2% L-glutamate (PAN-Biotech GmbH, Aidenbach, Germany), 1% penicillin/streptomycin (Capricorn Scientific GmbH, Ebsdorfergrund, Germany) and 10% FCS (Thermo Fisher Scientific, Waltham, USA) and cultured on 3µg/cm² fibronectin-coated plates (Sigma-Aldrich, Burlington, USA).

3-(4,5-dimethylthiazol-2-yl)-2,5-diphenyltetrazolium bromide (MTT) assay

MTT metabolic assay was used to evaluate the metabolic activity after 24 h incubation with ECVE or CSE according the manufacturer’s protocol (Sigma-Aldrich, Burlington, USA).

LDH cytotoxicity assay

24 h after seeding, cells were treated with ECVE, NF ECVE or CSE for 24 h. Twenty-four hours after treatment with different doses of ECVE, NF ECVE or CSE, the CyQUANT™ LDH Cytotoxicity Assay (Thermo Fisher Scientific, Waltham, USA) was performed using 50µl cell medium collected from the samples according to the manufacturer's instructions. Control cells were treated with a medium without ECVE, NF ECVE or CSE.

Proliferation assay

Cells were cultured in 24-well plates. Twenty-four hours after seeding, cells were treated with different doses of ECVE, NF ECVE or CSE and simultaneously incubated with bromodeoxyuridine [BrdU (colorimetric) Cell Proliferation ELISA] assay (Roche, Basel, Switzerland) for 24 h according to the manufacturer's instructions. To quantify proliferation, absorbance was measured with a microplate reader (Tecan Group Ltd, Männedorf, Switzerland) at 370 nm (absorbance at 450 nm was measured as a reference). Control cells were treated with a medium without ECVE, NF ECVE or CSE.

Wound healing assay

Culture-inserts (Ibidi culture-inserts, 2-well) were inserted into the bottom of 24-well plates to provide two cell culture reservoirs and 2,500 hPASMC and 5,000 mPASMC were seeded per reservoir. The wound healing assay was initiated by removing the culture-insert 24 h after seeding. Subsequently, the cells were treated with different doses of ECVE, NF ECVE or CSE for 16 h. Control cells were treated with a medium without ECVE, NF ECVE or CSE. Simultaneously with the application of ECVE, NF ECVE, CSE or the control medium, the wound closure (cell migration) was recorded

using an IncuCyte ZOOM™ live cell imaging system (Essen BioScience, Inc., Ann Arbor, USA) and pictures were acquired every hour for 16 h. This system measured scratch closure in real-time and automatically calculated the relative wound density within the initially vacant area at each time point.

Apoptosis assay

For the assessment of apoptosis, an IncuCyte ZOOM (Essen BioScience Inc.) system and an annexin XII-based polarity-sensitive probe from Kinetic Apoptosis Kit (#ab129817, Abcam, Cambridge, UK) were used according to the manufacturer's instructions. Twenty-four hours after seeding, cells were treated with different doses of ECVE, NF ECVE or CSE for 24 h. Control cells were treated with a medium without ECVE, NF ECVE or CSE. Twenty-four hours after exposure of the cells to ECVE, NF ECVE, CSE or the control medium, the fluorescent signal from the annexin XII-based polarity-sensitive probe was measured at an excitation wavelength of 488 nm and an emission wavelength of 530 nm.

Dead cell count

To determine dead cells, 10,000 cells/well of mPASMC and hPASMC were seeded in a 96-well plate. Twenty-four hours after seeding, cells were treated with different doses of ECVE, NF ECVE or CSE for 24 h. Control cells were treated with a medium without ECVE, NF ECVE or CSE. Twenty-four hours after exposure to ECVE, NF ECVE, CSE or the control medium, the fluorescent signal from BOBO™-3 Iodide (Thermo Fisher Scientific, Waltham, USA) was collected by an IncuCyte ZOOM and analysed using the Incucyte® integrated analysis software (Essen BioScience Inc., Ann Arbor, USA). BOBO™-3 Iodide penetrates cells with diminished plasma membrane integrity, resulting in a 100–1000-fold increase in fluorescence upon binding to DNA.

Quantitative real-time PCR

Quantitative real-time PCR of mPASMC and mATII cells was performed 24 h after exposure of the cells to different doses of ECVE, NF ECVE or the control medium (medium without ECVE and NF ECVE). Cells were treated with ECVE, NF ECVE, CSE or the control medium 24 h after seeding. The mRNA was isolated from the mPASMC and mATII by using the RNeasy Mini Kit (Qiagen, Hilden, German) according to the manufacturer's instructions. The 1,000ng mRNA was used to synthesise cDNA with the iScript cDNA Synthesis Kit (Bio-Rad Laboratories GmbH, Feldkirchen, Germany). Quantitative real-time PCR was performed with the iQ™ SYBR® Green Supermix (Bio-Rad Laboratories GmbH, Feldkirchen, Germany) according to the manufacturer's instructions.

All primers used in the current study are listed in Supplemental Table 1. Expression levels of target genes were normalised by concurrent measurement of the reference gene *beta-2-microglobulin* (*B2M*).

Supplemental Table 1.

Primer	Sequences
B2M (Beta2-microglobulin)	AGCCCAAGACCGTCTACTGG
	TTCTTTCTGCGTGCATAAATTG
Bcl2 (B cell leukemia/lymphoma 2)	TGGGATGCCTTTGTGGAACT
	TTGGCAATTCCTGGTTCGGT
Ccna1 (Cyclin A1)	AAGAACCTGAGAAGCAGGGC
	CAGGGTCTCTGTGCGAAGTT
Nos2 (Inducible nitric oxide synthase)	TGATGTGCTGCCTCTGGCT
	AATCTCGGTGCCCATGTACC
Mmp9 (Matrix metallopeptidase 9)	CAGCCGACTTTTGTGGTCTTC
	GTCGAAATGGGCATCTCCCT
Timp3 (Tissue inhibitor of metalloproteinase 3)	TCCAAACACTACGCCTGCAT
	CTGCTTGCTGCCTTTGACTG
Traf1 (TNF receptor-associated factor 1)	GCGCACAGTGTGAGAAGAGA
	AGAGAACTCTGGGCTCCGAT

Microarray experiments

Twenty-four hours after exposure of the cells to ECVE, NF ECVE or control medium (medium without ECVE and NF ECVE), microarray analysis (GEO accession number GSE202215) of mPASMC and mATII cells was performed (project number GEn-1543) by using oligonucleotide spotted microarray slides (Agilent Technologies, Santa Clara, USA). Purified total RNA was amplified and Cy3-labelled using the LIRAK kit (Agilent Technologies, Santa Clara, USA) following the kit instructions. 200ng of total RNA was used per reaction. The Cy-labelled aRNA was hybridised overnight to 8x60K 60 mer oligonucleotide spotted microarray slides (design ID 028005). Hybridisation and subsequent washing and drying of the slides were performed following the Agilent hybridisation protocol. The dried slides were scanned at 2µm/pixel resolution using the InnoScan 900 (Innopsys, Carbonne, France). Image analysis was performed with the Mapix 6.5.0 software, and calculated values for all spots were saved as GenePix results files. The data were evaluated using the R-software (R 3.5.1) and the limma package (limma 2.14) from BioConductor. Log mean spot signals were taken for further analysis. Data were background corrected using the NormExp procedure on the negative control spots and quantile-normalised before averaging [3]. Genes were ranked for differential expression using a moderated t-statistic. Pathway analyses were done using gene set tests on the ranks of the t-values.

Protein isolation and Western blot analysis

Western blot analysis was performed using mPASMC lysates after exposure of the cells to ECVE, NF ECVE or control medium (medium without ECVE and NF ECVE) for 24 h. Cells were treated with ECVE, NF ECVE, CSE or control medium 24 h after seeding. The blots were blotted for ubiquitin-binding protein p62 (p62, SPC-219,

StressMarq Biosciences, Victoria, Canada), microtubule-associated proteins 1A/1B light chain 3B (LC3II, # SPC-217, StressMarq Biosciences, Victoria, Canada), PCNA (#13110, RRID: AB_2636979, Cell Signaling, Danvers, CA, USA). The protein expression level of β-actin (#A5316; RRID: AB_476743, Sigma-Aldrich, Burlington, USA) was used as the loading control. The dilution of primary antibodies was 1:1,000 for p62, LC3II and PCNA and 1:50,000 for β-actin. The dilution of the corresponding secondary antibodies was 1:5,000. The incubation time for the primary antibodies was overnight at 4°C and 1h at room temperature for the corresponding secondary antibodies.

Glutathione assay

Total glutathione (GSH and GSH/GSSG ratios) was measured in mATII cell lysates after exposure to ECVE, or NF ECVE, CSE or control medium (medium without ECVE and NF ECVE) for 24 h by a GSH/GSSG-Glo™ assay (Promega, Madison, United States) following the manufacturer's instructions. Luminescence was measured by a microplate reader (Tecan Group Ltd, Männedorf, Switzerland). Cells were treated with ECVE, NF ECVE, CSE or control medium 24 h after seeding.

E-cigarette vapor application in isolated ventilated and perfused mouse lungs

To isolate the lungs, mice were intubated through a tracheostomy under deep anaesthesia with ketamine (100mg/kg body weight, i.p.) and xylazine (20mg/kg body weight, i.p.) after anticoagulation with heparin (2,500U/kg body weight). Mice were ventilated with a normoxic gas mixture (21.0% O_2, 5.3%CO_2, balanced with N_2, 10µl/g body weight tidal volume, 90 breaths/min and 3 cm H_2O positive end expiratory pressure) using a piston pump (Minivent Type 845, Hugo Sachs Elektronik, March-Hugstetten, Germany) while the chest was opened and the lung and heart were

prepared. Lung perfusion with Krebs-Henseleit buffer [120 mM NaCl, 4.3 mM KCl, 1.1 mM KH_2PO_4, 2.4 mM $CaCl_2$, 1.3 mM $MgCl_2$, 13.3 mM glucose, 5% (w/v) hydroxyethyl amylopectin (molecular weight 200,000Da)] was initiated through a catheter inserted into the pulmonary artery using a peristaltic pump (ISM834A V2.10, Ismatec, Wertheim, Germany). After the lung and heart removal from the chest cavity, the lung/heart preparation was freely suspended on a scale to measure its weight changes, and a catheter was inserted in the left atrium for collection of the outflow perfusate (Supplementary methods figure 1). Outflow pressure was fixed at 2 cm H_2O. Pulmonary arterial pressure, pulmonary venous pressure, ventilation pressure and weight were monitored continuously during the experiment.

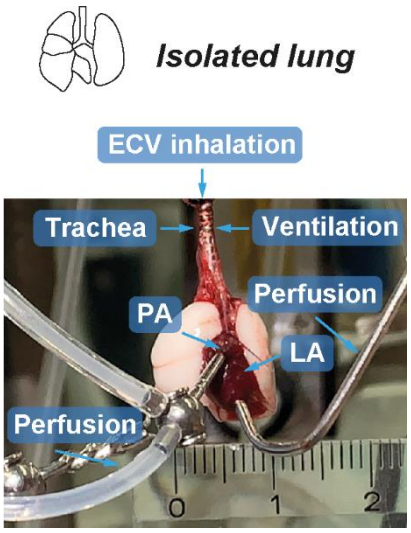

Supplementary methods figure 1. Experimental setup. Nicotine-containing e-cigarette vapour (ECV) was applied in a repetitive manner 3 times for 5 min each, via the trachea in the isolated ventilated and perfused mouse lung system. The lung was ventilated via the trachea and perfused via the pulmonary artery (PA) with recirculating the perfusate by a catheter in the left atrium (LA).

After preparation of the lung and an initial steady-state perfusion period, the lungs were ventilated five times for 10 min with a hypoxic gas mixture (1% O_2, 5.3% CO_2, balanced

with N_2) to determine HPV, each time followed by a ventilation period with a normoxic gas mixture (21% O_2, 5.3% CO_2, balanced with N_2). The normoxic interval between the first and second hypoxic manoeuvre was 25 min; subsequent interval durations lasted 50 min. The K_{fc} was determined by increasing the venous pressure from 2 to 12cm H_2O for 8 min ("pressure challenge"). The first pressure challenge was performed during normoxic ventilation 7 min after the first hypoxic manoeuvre and was used as a reference for all subsequent pressure challenges. After the second hypoxic manoeuvre (which was used as a reference for all ensuing hypoxic manoeuvres), the following protocol was applied to the lung 3 times: 1) normoxic ventilation stage: 10 min of ventilation, intratracheal application of ECV or NF ECV for 5 min, followed by 17 min of ventilation, 8 min of pressure challenge and 10 min of ventilation; 2) subsequent hypoxic ventilation stage: 10 min of ventilation. ECV or NF ECV was produced by Joyetech eVic Primo Mini e-cigarette (0.56Ohm, 4.1V, 30W, Joyetech, Riccardo Retail GmbH, Neubrandenburg, Germany) and drawn with normoxic air into a perfusor syringe using a vacuum pump (see Supplementary methods figure 2). The puffing condition was 4 puffs of 5 sec duration (20 sec in total). For the application of ECV or NF ECV in the isolated lung, the vapour was delivered via the inspiratory tube by a syringe driver, mimicking the ventilation mode of vapour-free ventilation. During the application, the expiratory tube of the ventilation was closed until the "normal" inspiratory volume was reached. After reaching the inspiratory volume, the expiratory tube was opened to release the ECV or NF ECV-air mixture. This procedure lasted 2 sec and was repeated 150 times for 5 min. Thus, ventilation with normoxic air was guaranteed during the intratracheal application of vapour. The PEEP (positive end-expiratory pressure) of 3cm H_2O was constant throughout the procedure. The same protocol was performed for control experiments, but only with normoxic air delivery without ECV or NF ECV. The strength of HPV was determined as the maximum

increase of PAP during hypoxia [1]. The K_{fc} was calculated from the slope of the lungs' weight gain induced by the increased lungs' fluid content during the pressure challenge [4].

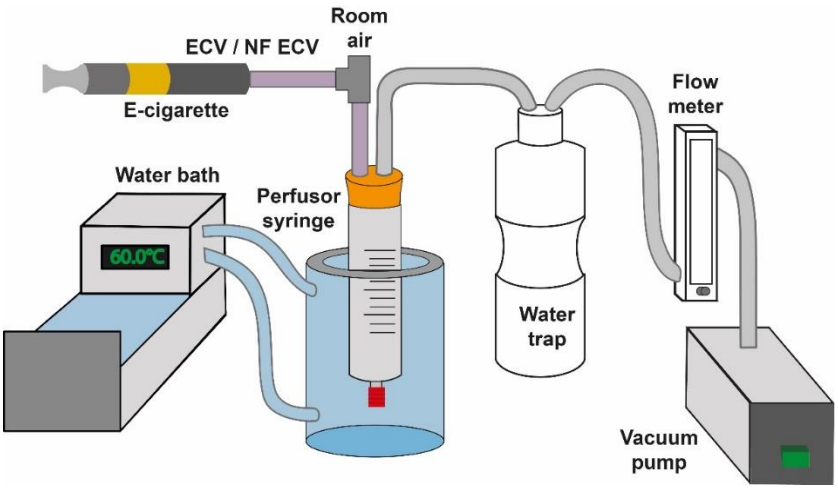

Supplementary methods figure 2. Preparation of e-cigarette vapour with or without nicotine (ECV or NF ECV) for inhalative application to the isolated lung via a syringe driver. Joyetech eVic-Primo Mini e-cigarettes were used to produce ECV or NF ECV. ECV or NF ECV was drawn into the syringe by a vacuum pump at a flow rate of 1000ml/min to a final volume of 50ml ECV or NF ECV. The puffing condition was four puffs of 5 sec each, 20 sec in total. The syringe was kept in a cylinder heated to 60°C to prevent condensation of the vapour until delivery to the lung. During the inhalation, the syringe containing ECV, NF ECV or normoxic air was kept under an ultraviolet light lamp to maintain a temperature of 37°C.

Animals for *in vivo* e-cigarette vapour exposure

Twelve mice per group were exposed to ECV, NF ECV or room air. All animals were used for the determination of *in vivo* hemodynamic and lung function measurements and for micro-computed tomography (µCT) imaging. Mice from each group were randomly assigned to echocardiography (n=7), histological (n=6), immunohistochemical (n=5-6), multiplex (n=10) and FACS (n=5) analyses. The number of experiments (n) for *in vivo* lung function and hemodynamics, echocardiography and µCT may differ from the initial n due to technical issues (e.g., dislocation of the measurement catheter).

Flow cytometry

Bronchoalveolar lavage (BAL) was collected, and the cell pellets were incubated with Fc block (Miltenyi Bitech, Bergisch Gladbach, Germany) and stained with CD45APC-Cy7 (clone 30-F11; BioLegend, Fell, Germany), CD11b Pacific Blue (clone M1/70; BioLegend, Fell, Germany), GR-1 PerCy7 (clone RB6-8C5; BioLegend, Fell, Germany), Ly6G FITC (clone 1A8, BioLegend, Fell, Germany) or SiglecF PE (clone E50/2440; BD Biosciences, Franklin Lakes, USA) anti-mouse antibodies in the dark for 15 min at 4°C; they were then washed with a fluorescence-activated cell sorting (FACS) buffer. Flow cytometry was performed with an LSRII flow cytometer (BD Biosciences, Franklin Lakes, USA) using the DIVA software (BD Biosciences, Franklin Lakes, USA) as previously described [5, 6]. The gating strategy was as follows: the total BAL cells were first gated with forward scatter (FSC) and side scatter (SSC). The lymphocytes were gated from the total BAL cells based on the low FSC and low SSC within the CD45+ cluster. The mononuclear phagocytes (MonPh) were gated based on the higher FSC and/or SSC within the CD45+ cluster. From the MonPh cluster, the $CD11c^{+}Gr\text{-}1^{-}$ population was sub-gated to differentiate resident macrophages (rAMs: $CD11b^{hi}Siglec\text{-}F^{hi}$) and exudate macrophages (ExMAs: $CD11b^{hi}SiglecF^{low}$). From the

MonPh cluster, the $CD11c^{-}Gr\text{-}1^{+}$ population was sub-gated to identify neutrophils ($GR\text{-}1^{+}Ly6G^{hi}$) and monocytes ($GR\text{-}1^{+}Ly6G^{-}$).

Multiplex assay

A custom-made mouse magnetic bead-based multiplex assay was used to analyse the levels of selected inflammatory mediators in BAL fluid (BALF) according to the manufacturer's protocol (R&D Systems, Minneapolis, USA). For the experiments, BALF was used after sedimentation of the cells by centrifugation at 300g for 10 min at 4°C). The assay was conducted using the Bio-Plex 200 instrument (Bio-Rad Laboratories GmbH, Feldkirchen, Germany) and analysed with the Bio-Plex Manager software (Bio-Rad Laboratories GmbH, Feldkirchen, Germany).

***In vivo* hemodynamics, echocardiography, histology and micro-computed tomography (µCT)**

Pulmonary vascular function was determined by *in vivo* haemodynamics using a Millar catheter (Model SPR-671 pressure catheter; Millar Instruments, Inc.; Houston, USA) and the PowerLab system with the LabChart 7.0 software (ADInstruments GmbH, Oxford, UK) [7]. Transthoracic echocardiography was performed using a VEVO770 or VEVO2100 system (Visualsonics, Toronto, Canada) [1].

For histological analysis, paraffin blocks were cut in 3µm sections, de-paraffinised, rehydrated, and stained with haematoxylin and eosin (H&E), following routine protocols. Septal wall thickness and mean linear intercept were assessed on H&E-stained slides using uniform random sampling and the Qwin alveolar morphometry software (Leica Microsystems, Wetzlar, Germany) as previously described[8].

In vivo µCT images were acquired using a Quantum GX micro-CT scanner (PerkinElmer, Waltham, USA) in mice under isoflurane anaesthesia. Reconstructed volumes were loaded into the Analyze Pro software (Analyze Direct, Overland Park, USA) and processed by a single observer. Lung segmentation and quantitative analysis of the CT density and functional residual capacity were performed as described previously [7].

In vivo lung function measurements

Measurements of *in vivo* lung function parameters were performed as previously described [9, 10] using the FlexiVent system equipped with an FX2 module (SCIREQ Scientific Respiratory Equipment Inc., Montreal, Canada) at a positive end-expiratory pressure (PEEP) of 3 cm H_2O, following the manufacturer's recommendations. Before the lung function measurement, deep inflation was performed by inflating the lung with air up to a pressure of 40 cm H_2O (from initially 3 cm H_2O) over 3 sec and then holding at 40 cm H_2O for an additional 3 sec [11]. This manoeuvre recruited closed lung areas, and the lung volume history was standardised [11-13]. The deep inflation manoeuvre was also used to determine the total inspiratory capacity. The overall respiratory system resistance, a single compartment model perimeter, was measured using a single frequency forced oscillation (SnapShot-150) perturbation as previously described [12]. The static compliance measurement was calculated from a respiratory pressure-volume (P-V) loop as previously described[12, 14]. The P-V manoeuvre included stepwise lung inflation through eight steps of increasing pressure from 3 to 40 cm H_2O with a 1-sec hold at each step. It was similarly followed by stepwise deflation back to the PEEP pressure of 3 cm H_2O. The whole manoeuvre lasted 16 sec. The P-V loop was constructed by recording volume changes and plotting it with pressure values at each holding step [12, 14]. The FlexiVent software automatically

calculated the lung function parameters associated with a perturbation. The software also provided a coefficient of determination (COD), which reflects the fit of the mathematical model to the dataset. Each dataset with an insufficient COD was labelled and excluded by the software as previously described [12]. The results were presented as an average of at least three repeated measurements with the COD above 0.90.

Exposure of mice to conventional cigarette smoke (CS)

Adult mice were exposed to mainstream smoke from 3R4F cigarettes (Kentucky University, Lexington, USA) produced by a smoke generator (Burkhart, Wedel, Germany) at a concentration of 140mg particulate matter/m^3 for 6 h as in [8, 9]. The blood samples to measure nicotine and cotinine concentration were taken immediately after removing the animals from the smoking chamber.

Plasma nicotine and cotinine concentration

Plasma nicotine and cotinine concentrations were measured after exposure of mice to ECV or CS for 6 h by liquid chromatography with tandem mass spectrometry by ABS Laboratories (Welwyn Garden City, UK). The samples to measure nicotine and cotinine concentration were taken immediately after removing the animals from the exposure chamber. Under deep anaesthesia with ketamine (100mg/kg body weight, i.p.) and xylazine (20mg/kg body weight, i.p.) after anticoagulation with heparin (2,500U/kg body weight), abdominal cavity of the mouse was opened and a blood sample was taken from abdominal aorta. Then the blood samples were centrifuged at 2000 g for 10 min (4°C).

Immunohistochemistry

Paraffin-embedded mouse lungs were cut into 3µm thick sections, deparaffinised and rehydrated following standard protocols. Antigen retrieval was performed using the Rodent Decloaker solution (Biocare Medical LLC, Pacheco, USA), and unspecific binding was blocked with a 10% BSA solution. The slides were incubated with primary antibodies (CD45: ab10559, Abcam Cambridge, UK; dilution 1:200 and CD3: #RBK 024-05, Zytomed Systems GmbH, Berlin, Germany; dilution 1:200) diluted in antibody diluent (Zytomed Systems GmbH, Berlin, Germany) overnight at 4°C. A ZytoChem Plus phosphatase polymer kit (Zytomed Systems GmbH, Berlin, Germany) and Warp Red Chromogen substrate kit (Zytomed Systems GmbH, Berlin, Germany) were used to visualise the staining according to the manufacturer's protocols. Counterstaining was performed with CAT Haematoxylin solution (Biocare Medical LLC, Pacheco, USA). The number of cells was determined in randomly selected fields using the Qwin software (Leica Microsystems, Wetzlar, Germany).

References:

1. Sommer N, Huttemann M, Pak O, Scheibe S, Knoepp F, Sinkler C, Malczyk M, Gierhardt M, Esfandiary A, Kraut S, Jonas F, Veith C, Aras S, Sydykov A, Alebrahimdehkordi N, Giehl K, Hecker M, Brandes RP, Seeger W, Grimminger F, Ghofrani HA, Schermuly RT, Grossman LI, Weissmann N. Mitochondrial Complex IV Subunit 4 Isoform 2 Is Essential for Acute Pulmonary Oxygen Sensing. *Circ Res* 2017: 121(4): 424-438.

2. Sun F, Xiao G, Qu Z. Isolation of Murine Alveolar Type II Epithelial Cells. *Bio Protoc* 2017: 7(10).

3. Silver JD, Ritchie ME, Smyth GK. Microarray background correction: maximum likelihood estimation for the normal-exponential convolution. *Biostatistics* 2009: 10(2): 352-363.

4. Seeger W, Walmrath D, Menger M, Neuhof H. Increased lung vascular permeability after arachidonic acid and hydrostatic challenge. *J Appl Physiol (1985)* 1986: 61(5): 1781-1789.

5. Peteranderl C, Morales-Nebreda L, Selvakumar B, Lecuona E, Vadasz I, Morty RE, Schmoldt C, Bespalowa J, Wolff T, Pleschka S, Mayer K, Gattenloehner S, Fink L, Lohmeyer J, Seeger W, Sznajder JI, Mutlu GM, Budinger GR, Herold S. Macrophage-epithelial paracrine crosstalk inhibits lung edema clearance during influenza infection. *J Clin Invest* 2016: 126(4): 1566-1580.

6. Herold S, Tabar TS, Janssen H, Hoegner K, Cabanski M, Lewe-Schlosser P, Albrecht J, Driever F, Vadasz I, Seeger W, Steinmueller M, Lohmeyer J. Exudate macrophages attenuate lung injury by the release of IL-1 receptor antagonist in gram-negative pneumonia. *Am J Respir Crit Care Med* 2011: 183(10): 1380-1390.

7. Kojonazarov B, Hadzic S, Ghofrani HA, Grimminger F, Seeger W, Weissmann N, Schermuly RT. Severe Emphysema in the SU5416/Hypoxia Rat Model of Pulmonary Hypertension. *Am J Respir Crit Care Med* 2019: 200(4): 515-518.

8. Seimetz M, Sommer N, Bednorz M, Pak O, Veith C, Hadzic S, Gredic M, Parajuli N, Kojonazarov B, Kraut S, Wilhelm J, Knoepp F, Henneke I, Pichl A, Kanbagli ZI, Scheibe S, Fysikopoulos A, Wu CY, Klepetko W, Jaksch P, Eichstaedt C, Grunig E, Hinderhofer K, Geiszt M, Muller N, Rezende F, Buchmann G, Wittig I, Hecker M, Hecker A, Padberg W, Dorfmuller P, Gattenlohner S, Vogelmeier CF, Gunther A, Karnati S, Baumgart-Vogt E, Schermuly RT, Ghofrani HA, Seeger W, Schroder K, Grimminger F, Brandes RP, Weissmann N. NADPH oxidase subunit NOXO1 is a target for emphysema treatment in COPD. *Nat Metab* 2020: 2(6): 532-546.

9. Hadzic S, Wu CY, Gredic M, Kojonazarov B, Pak O, Kraut S, Sommer N, Kosanovic D, Grimminger F, Schermuly RT, Seeger W, Bellusci S, Weissmann N. The effect of long-term doxycycline treatment in a mouse model of cigarette smoke-induced emphysema and pulmonary hypertension. *Am J Physiol Lung Cell Mol Physiol* 2021: 320(5): L903-L915.

10. Gouveia L, Kraut S, Hadzic S, Vazquez-Liebanas E, Kojonazarov B, Wu CY, Veith C, He L, Mermelekas G, Schermuly RT, Weissmann N, Betsholtz C, Andrae J. Lung developmental arrest caused by PDGF-A deletion: consequences for the adult mouse lung. *Am J Physiol Lung Cell Mol Physiol* 2020: 318(4): L831-L843.

11. Boucher M, Henry C, Khadangi F, Dufour-Mailhot A, Tremblay-Pitre S, Fereydoonzad L, Brunet D, Robichaud A, Bosse Y. Effects of airway smooth muscle contraction and inflammation on lung tissue compliance. *Am J Physiol Lung Cell Mol Physiol* 2022: 322(2): L294-L304.

12. McGovern TK, Robichaud A, Fereydoonzad L, Schuessler TF, Martin JG. Evaluation of respiratory system mechanics in mice using the forced oscillation technique. *J Vis Exp* 2013(75): e50172.

13. Zosky GR, Janosi TZ, Adamicza A, Bozanich EM, Cannizzaro V, Larcombe AN, Turner DJ, Sly PD, Hantos Z. The bimodal quasi-static and dynamic elastance of the murine lung. *J Appl Physiol (1985)* 2008: 105(2): 685-692.

14. Bates JHT. Lung mechanics: an inverse modeling approach. Cambridge University Press, Cambridge, UK; New York, 2009.

a)

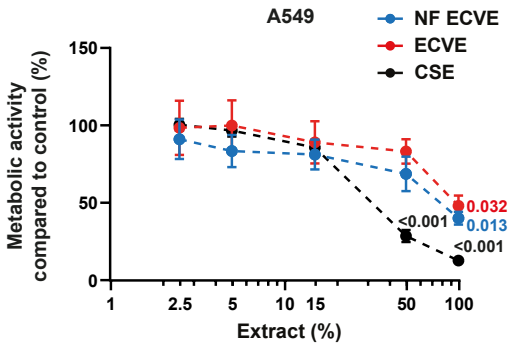

b)

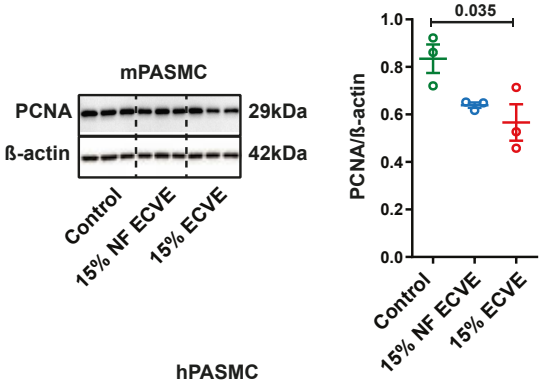

c)

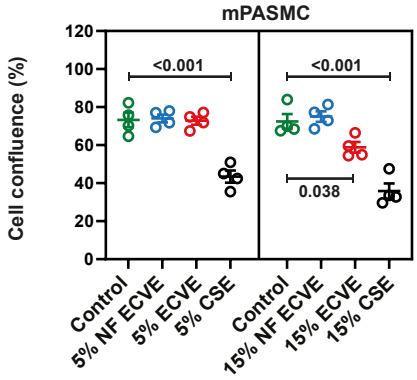

d)

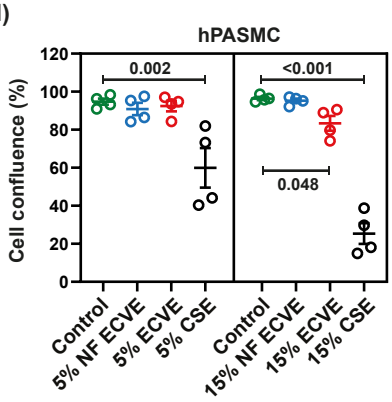

e i)

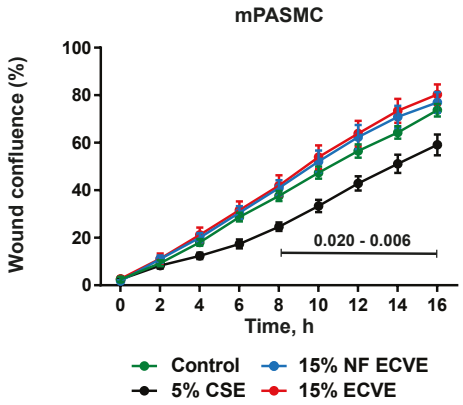

e ii)

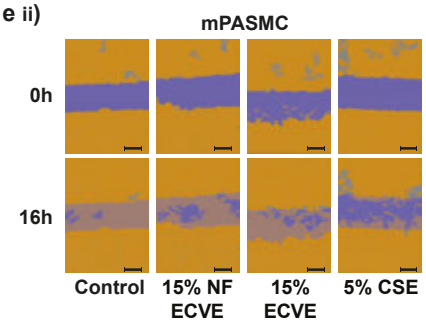

f i)

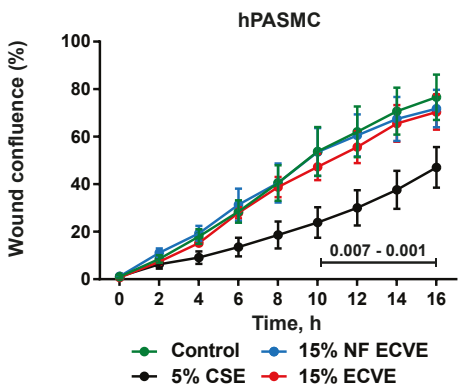

f ii)

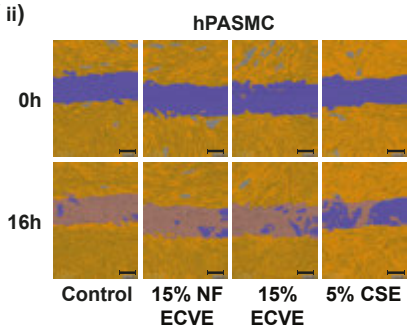

g)

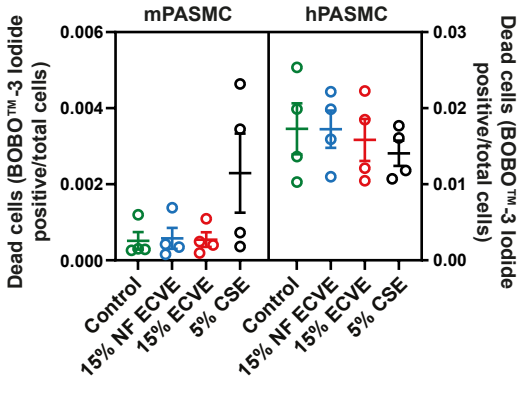

Supplementary Figure 1. Effect of *in vitro* ECVE or NF ECVE exposure on metabolic activity, cell confluence, PCNA protein expression and migration.

a) Cell metabolic activity of human epithelial cells from A549 cell line (n=5) after exposure to different concentrations of either nicotine-free e-cigarette vapour extract (NF ECVE), nicotine-containing e-cigarette vapour extract (ECVE) or conventional cigarette smoke extract (CSE). Data are presented as percent of control. Significant p-values in comparison to control. **b**) Protein expression of PCNA normalised to expression of β-actin in mPASMC exposed to either 15% NF ECVE or 15 % ECVE (n=3). **c-d**) Cell confluence (n=4 each) of mPASMC and hPAMSC exposed to either NF ECVE, ECVE or CSE. **e, f**) Wound confluence (% of confluence at 0h) of mPASMC (**e i**, n=10) and hPASMC (**f i**, n=5) after exposure to either 15% NF ECVE, 15% ECV, 5% CSE or control. Depicted are representative pictures of wound healing assays, used for determination of cell migration (**e ii, f ii**). Scale bars 300µm. **g**) Dead cell counts (n=4 each) for mPASMC and hPAMSC exposed to either NF ECVE, ECVE or CSE.

Controls were treated with medium without ECVE, NF ECVE or CSE. n for mPASMC, and hPASMC represent independent cell isolations per group, n for A549 cells represent independent experiments per group. Statistical analysis was performed by one-way ANOVA with Tukeys post hoc-test. Data are presented as mean ± SEM.

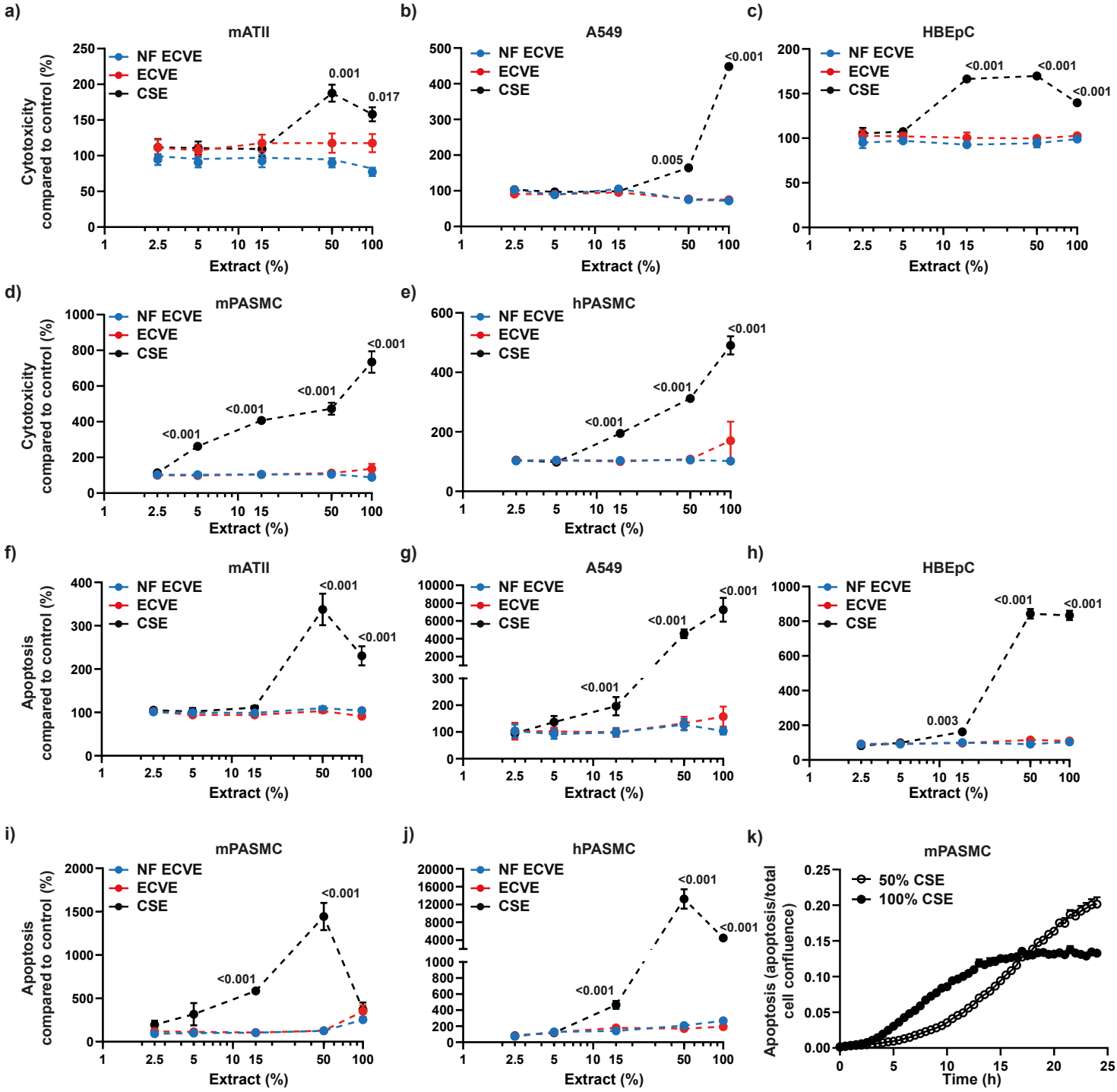

Supplementary Figure 2. Effect of *in vitro* ECVE or NF ECVE exposure on cytotoxicity and apoptosis.
a-e) Cytotoxicity assays of primary mouse ATII cells (**a**, mATII, n=3), A549 cells (**b**, n=3), HBEpC (**c**, n=3), primary mPASMC (**d**, n=3), and primary hPASMC (**e**, n=3). **f-j**) Apoptosis assays of mATII cells (**f**, n=5), A549 cells (**g**, n=4), HBEpC (**h**, n=4), mPASMC (**i**, n=4), hPASMC (**j**, n=4). Cells were either exposed to nicotine-free e-cigarette vapour extract (NF ECVE), nicotine-containing e-cigarette vapour extract (ECVE) or conventional cigarette smoke extract (CSE). **k**) Kinetics of apoptosis in mPASMC exposed to 50% and 100% CSE (n=4).
Controls were treated with medium without ECVE, NF ECVE or CSE. n for mATII cells, mPASMC, and hPASMC represent independent cell isolations per group, n for A549 cells and HBEpC represent independent experiments per group. Statistical analysis was performed by one-way ANOVA with Tukeys post hoc-test. Significant p-values in comparison to CSE are presented. Data are presented as mean ± SEM.

In vitro

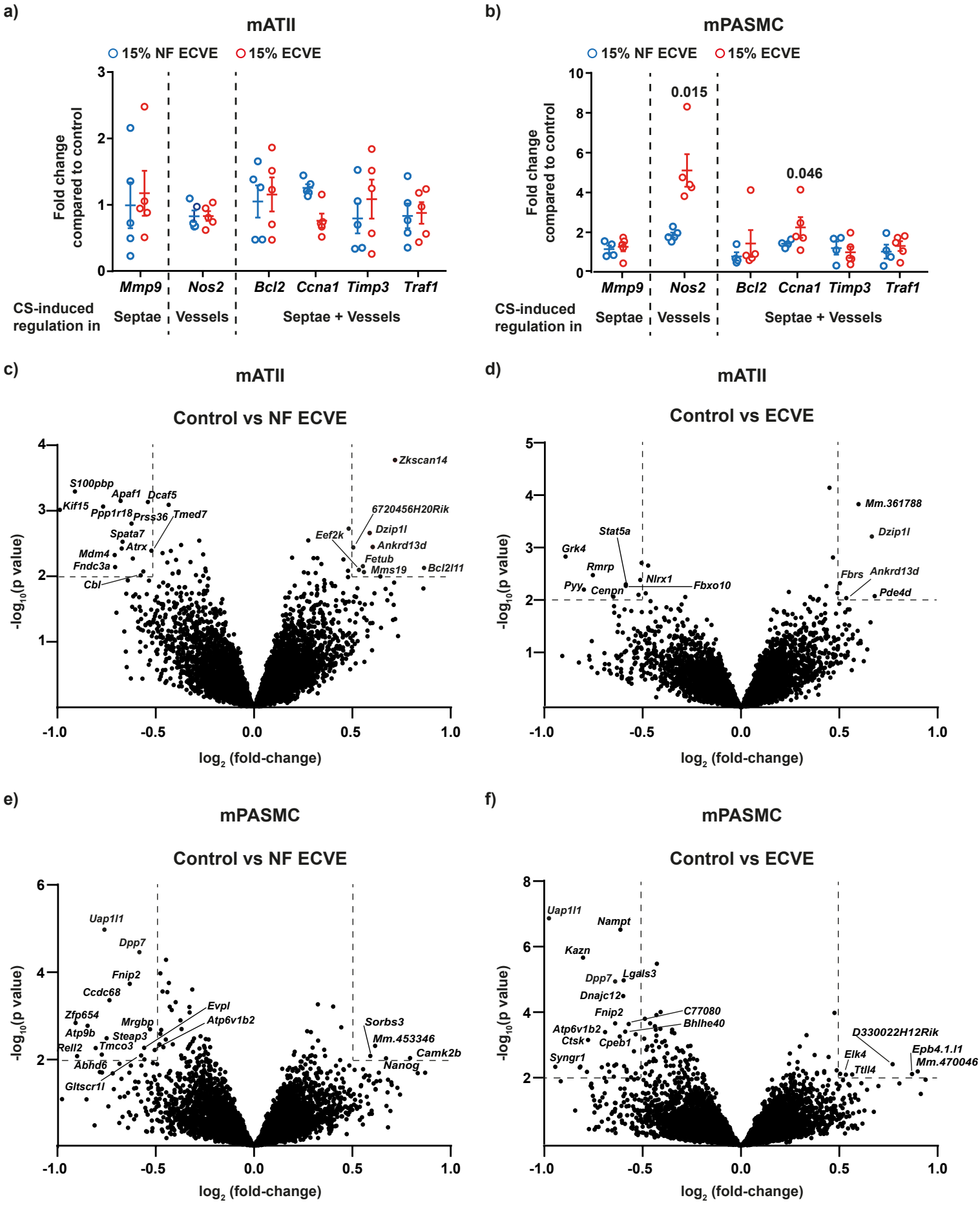
a)
mATII
15% NF ECVE
15% ECVE
Fold change compared to control
Mmp9
Nos2
Bcl2
Ccna1
Timp3
Traf1
CS-induced regulation in
Septae
Vessels
Septae + Vessels
b)
mPASMC
0.015
0.046
c)
mATII
Control vs NF ECVE
-log10(p value)
log2 (fold-change)
Zkscan14
S100pbp
Apaf1
Dcaf5
Kif15
Ppp1r18
Prss36
Tmed7
6720456H20Rik
Spata7
Eef2k
Dzip1l
Atrx
Ankrd13d
Mdm4
Fetub
Fndc3a
Mms19
Bcl2l11
Cbl
d)
mATII
Control vs ECVE
Mm.361788
Dzip1l
Stat5a
Grk4
Rmrp
Fbrs
Ankrd13d
Nlrx1
Pyy
Cenpn
Fbxo10
Pde4d
e)
mPASMC
Control vs NF ECVE
Uap1l1
Dpp7
Fnip2
Ccdc68
Evpl
Zfp654
Mrgbp
Atp6v1b2
Atp9b
Steap3
Sorbs3
Rell2
Tmco3
Mm.453346
Camk2b
Abhd6
Nanog
Gltscr1l
f)
mPASMC
Control vs ECVE
Uap1l1
Nampt
Kazn
Dpp7
Lgals3
Dnajc12
Fnip2
C77080
Atp6v1b2
Bhlhe40
Ctsk
Cpeb1
D330022H12Rik
Epb4.1.l1
Syngr1
Elk4
Mm.470046
Ttll4

Supplementary Figure 3. Gene expression patterns of ECVE- or NF ECVE-exposed cells from real-time PCR and microarray analyses.

a, b) Real-time PCR analysis of mRNA expression of *Mmp9, Nos2, Bcl2, Ccna1, Timp3* and *Traf1* in primary mouse mATII cells (**a**, n=5) and primary mPASMC (**b**, n=4-5) after exposure to either 15% nicotine-free e-cigarette vapour extract (NF ECVE) or 15% nicotine-containing e-cigarette vapour extract (ECVE). Data are presented as fold change compared to respective untreated controls. Statistical analysis was performed by Student's t-test. Data are presented as mean ± SEM.

c-f) Volcano plots of microarray analyses from primary mATII cells (**c, d,** n=8) and mPASMC (**e, f**, n=8) exposed to 15% NF ECVE or 15% ECVE. The y-axis [$-\log_{10}$(p value)] displays the significance level and the x-axis [$\log_2$ (fold-change)] the fold change compared to control. Controls were treated with medium without ECVE or NF ECVE. n represents independent cell isolations per group.

Abbreviation: *Abhd6* – abhydrolase domain containing 6; *Ankrd13d* – ankyrin repeat domain 13 family, member D; *Apaf1* – apoptotic peptidase activating factor 1; *Atp6v1b2* – ATPase, H^+ transporting, lysosomal V1 subunit B2; *Atp9b* – ATPase, class II, type 9B; *Atrx* – alpha thalassemia/mental retardation syndrome X-linked homolog (human); *Bcl-2* – B-cell lymphoma 2; *Bhlhe40* – basic helix-loop-helix family, member e40; *C77080* – expressed sequence C77080; *Camk2b* – calcium/calmodulin-dependent protein kinase II, beta; *Ccdc68* – coiled-coil domain containing 68; *Ccna1* – Cyclin A1; *Cenpn* – centromere protein N; *Cpeb1* – cytoplasmic polyadenylation element binding protein 1; *Ctsk* – cathepsin K; *Dcaf5* – DDB1 and CUL4 associated factor 5; *Dnajc12* – DnaJ (Hsp40) homolog, subfamily C, member 12; *Dpp7* – dipeptidylpeptidase 7; *Dzip1l* – DAZ interacting protein 1-like; *Elk4* – ELK4, member of ETS oncogene family; *Evpl* – envoplakin; *Fbrs* – fibrosin; *Fbxo10* – F-box protein 10; *Fndc3a* – fibronectin type III domain containing 3A; *Fnip2* – folliculin interacting protein 2; *Gltscr1l* – glioma tumor suppressor candidate region gene 1-like; *Grk4* – G protein-coupled receptor kinase 4; *Kazn* – kazrin, periplakin interacting protein; *Kif15* – kinesin family member 15; *Lgals3* – lectin, galactose binding, soluble 3; *Mdm4* – transformed mouse 3T3 cell double minute 4; *Mmp9* – matrix metalloproteinase 9; *Mrgbp* – MRG/MORF4L binding protein; *Nampt* – nicotinamide phosphoribosyltransferase; *Nanog* – Nanog homeobox; *Nos2* – nitric oxide synthase 2; *Pde4d* – phosphodiesterase 4D, cAMP specific; *Ppp1r18* – protein phosphatase 1, regulatory subunit 18; *Prss36* – protease, serine, 36; *Pyy* – peptide YY; *Rell2* – RELT-like 2; *Rmrp* – RNA component of mitochondrial RNAase P; *S100pbp* – S100P binding protein; *Sorbs3* – sorbin and SH3 domain containing 3; *Spata7* – spermatogenesis associated 7; *Stat5a* – signal transducer and activator of transcription 5A; *Steap3* – STEAP family member 3; *Syngr1* – synaptogyrin 1; *Timp3* – tissue inhibitor of metalloproteinase 3; *Tmco3* – transmembrane and coiled-coil domains 3; *Tmed7* – transmembrane emp24 protein transport domain containing 7; *Traf1* – TNF receptor-associated factor 1; *Ttll4* – tubulin tyrosine ligase-like family, member 4; *Uap1l1* – UDP-N-acetylglucosamine pyrophosphorylase 1-like 1; *Zfp654* – zinc finger protein 654.

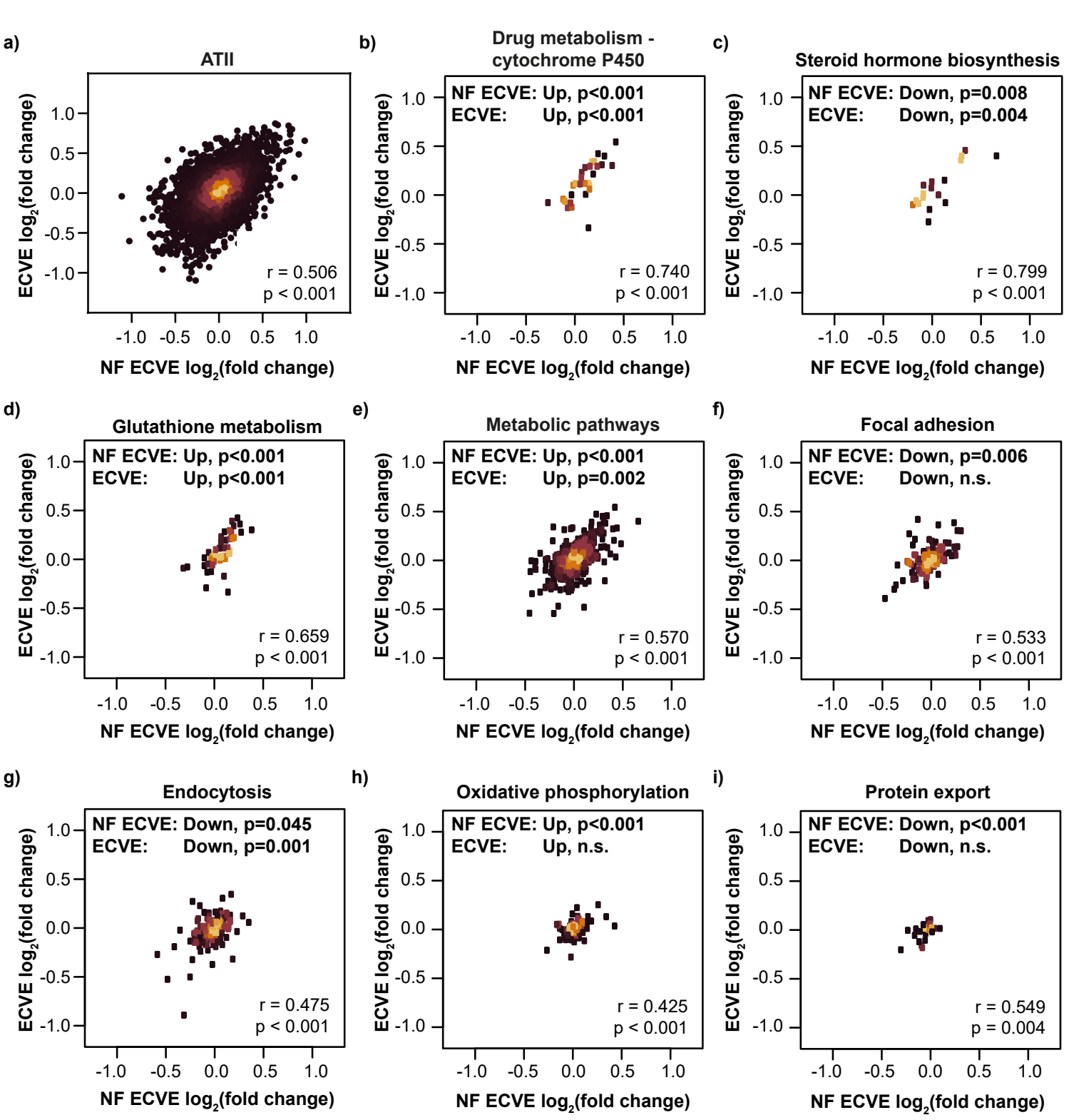

Supplementary Figure 4. Comparison of gene expression patterns of mouse alveolar epithelial type II cells (mATII) exposed to ECVE or NF ECVE from microarray analyses.

a-i) Correlation of mRNA transcript expression of microarray data between primary mATII cells either exposed to 15% nicotine-free e-cigarette vapour extract (NF ECVE) or 15% nicotine-containing e-cigarette vapour extract (ECVE). Controls were treated with medium without ECVE or NF ECVE. Data show all measured mRNA transcripts (**a**), or the subsets of the data from genes being annotated to KEGG pathways: "Drug metabolism – cytochrome" p450 (**b**), "Steroid hormone biosynthesis" (**c**), "Glutathione metabolism" (**d**), "Metabolic pathways" (**e**), "Focal adhesion" (**f**), "Endocytosis" (**g**) "Oxidative phosphorylation" (**h**), and "Protein export" (**i**). The colour of the points indicates the spatial density of the values (lowest density is black, highest density is yellow). The densities were obtained using a 2-dimensional Gaussian kernel estimator. The colouring visualizes the inner structure of dense clouds of overplotted points. "Up" and "Down" indicate up- or downregulation of the majority of respective mRNA transcripts in the specific pathway. n.s., not significant changes. Data are derived from n=8 independent cell isolations per group.

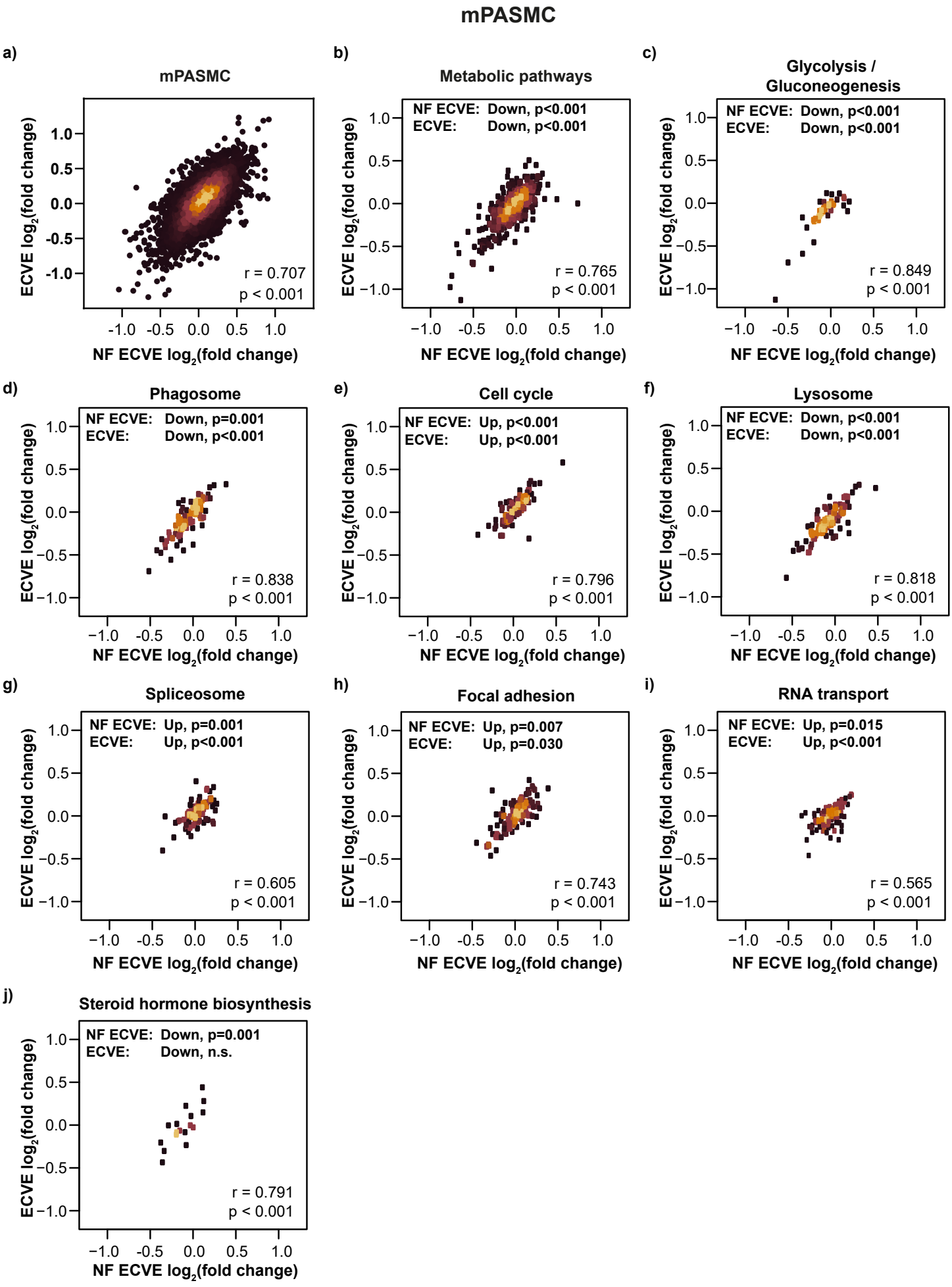
mPASMC
a)
mPASMC
r = 0.707
p < 0.001
b)
Metabolic pathways
NF ECVE: Down, p<0.001
ECVE: Down, p<0.001
r = 0.765
p < 0.001
c)
Glycolysis / Gluconeogenesis
NF ECVE: Down, p<0.001
ECVE: Down, p<0.001
r = 0.849
p < 0.001
d)
Phagosome
NF ECVE: Down, p=0.001
ECVE: Down, p<0.001
r = 0.838
p < 0.001
e)
Cell cycle
NF ECVE: Up, p<0.001
ECVE: Up, p<0.001
r = 0.796
p < 0.001
f)
Lysosome
NF ECVE: Down, p<0.001
ECVE: Down, p<0.001
r = 0.818
p < 0.001
g)
Spliceosome
NF ECVE: Up, p=0.001
ECVE: Up, p<0.001
r = 0.605
p < 0.001
h)
Focal adhesion
NF ECVE: Up, p=0.007
ECVE: Up, p=0.030
r = 0.743
p < 0.001
i)
RNA transport
NF ECVE: Up, p=0.015
ECVE: Up, p<0.001
r = 0.565
p < 0.001
j)
Steroid hormone biosynthesis
NF ECVE: Down, p=0.001
ECVE: Down, n.s.
r = 0.791
p < 0.001
ECVE log2(fold change)
NF ECVE log2(fold change)

Supplementary Figure 5. Comparison of gene expression patterns of mouse pulmonary arterial smooth muscle cells (mPASMC) treated with ECVE or NF ECVE from microarray analyses.

a-j) Correlation of mRNA transcript expression of microarray data between primary mPASMC cells either exposed to 15% nicotine-free e-cigarette vapour extract (NF ECVE) or 15% nicotine-containing e-cigarette vapour extract (ECVE). Controls were treated with medium without ECVE or NF ECVE. Data show measured mRNA transcripts (**a**), or the subsets of the data from genes being annotated to KEGG pathways: “Metabolic pathways”(**b**), “Glycolysis/Gluconeogenesis” (**c**), “Phagosome” (**d**), “Cell cycle” (**e**), “Lysosome” (**f**), “Spliceosome” (**g**) “Focal adhesion” (**h**), “RNA transport” (**i**) and “Steroid hormone biosynthesis” (**j**). The colour of the points indicates the spatial density of the values (lowest density is black, highest density is yellow). The densities were obtained using a 2-dimensional Gaussian kernel estimator. The colouring visualizes the inner structure of dense clouds of overplotted points. “Up” and “Down” indicate up- or downregulation of the majority of respective mRNA transcripts in the specific pathway. n.s., not significant changes. Data are derived from n=8 independent cell isolations per group.

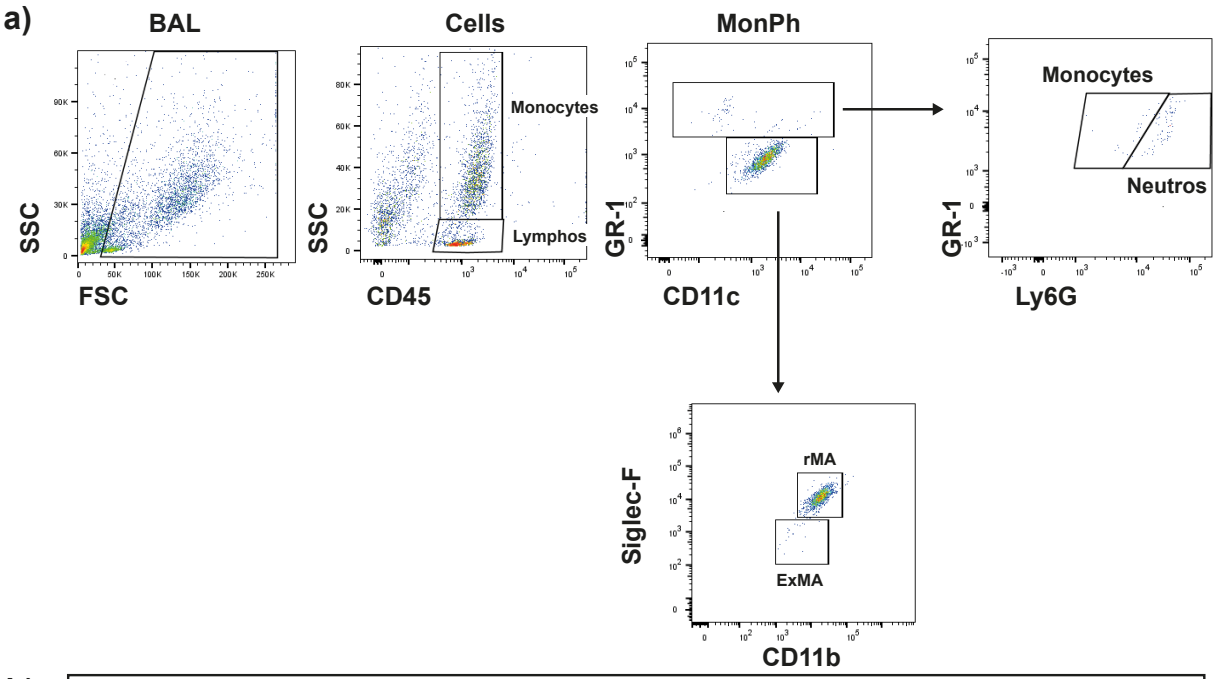
a)
BAL
Cells
MonPh
SSC
FSC
SSC
CD45
Monocytes
Lymphos
GR-1
CD11c
Monocytes
Neutros
GR-1
Ly6G
Siglec-F
CD11b
rMA
ExMA

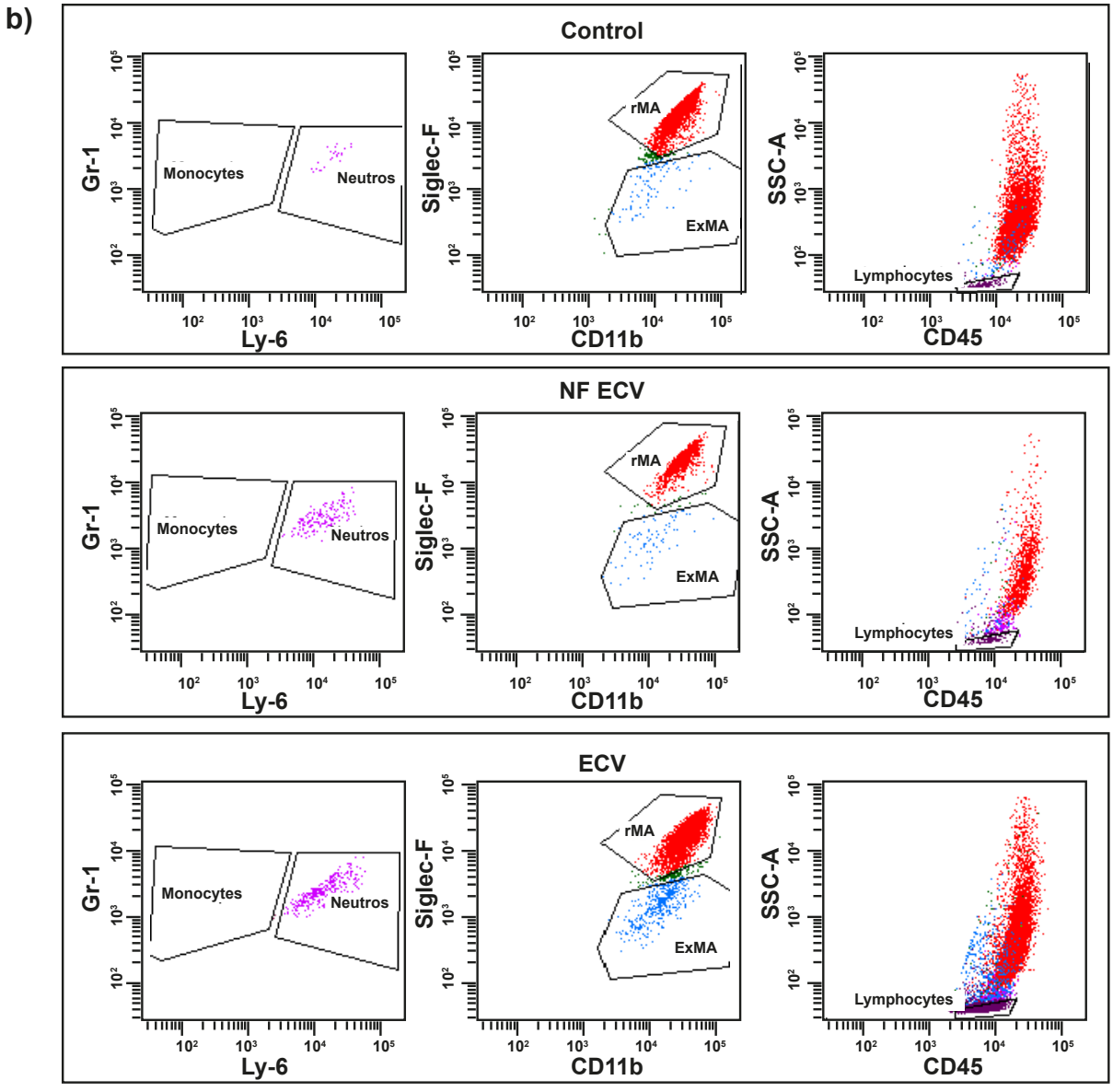
b)
Control
NF ECV
ECV
Gr-1
Ly-6
Monocytes
Neutros
Siglec-F
CD11b
rMA
ExMA
SSC-A
CD45
Lymphocytes

Supplementary Figure 6. Effect of long-term *in vivo* exposure to ECV or NF ECV on immune cell composition of bronchoalveolar lavage (BAL).

a) Flow cytometry gating strategy. First, the total BAL cells were gated with forward scatter (FSC) and side scatter (SSC). From the total BAL cells, the lymphocytes were gated based on low FSC and low SSC within the CD45+ cluster. The mononuclear phagocytes (MonPh) were gated based on the higher FSC and/or SSC within the CD45+ cluster. From the MonPh cluster, the $CD11c^{+}Gr\text{-}1^{-}$ population was sub-gated to differentiate resident macrophages (rAMs: $CD11b^{hi}Siglec\text{-}F^{hi}$) and exudate macrophages (ExMAs: $CD11b^{hi}Siglec\text{-}F^{low}$). From the MonPh cluster, the $CD11c^{-}Gr\text{-}1^{+}$ population was sub-gated to identify neutrophils ($GR\text{-}1^{+}Ly6G^{hi}$) and monocytes ($GR\text{-}1^{+}Ly6G^{-}$).

b) Representative flow cytometry plots of the bronchoalveolar lavage (BAL) from mice exposed to either nicotine-free e-cigarette vapour (NF ECV) or nicotine-containing e-cigarette vapour (ECV) for 8 months. Control animals received room air only.

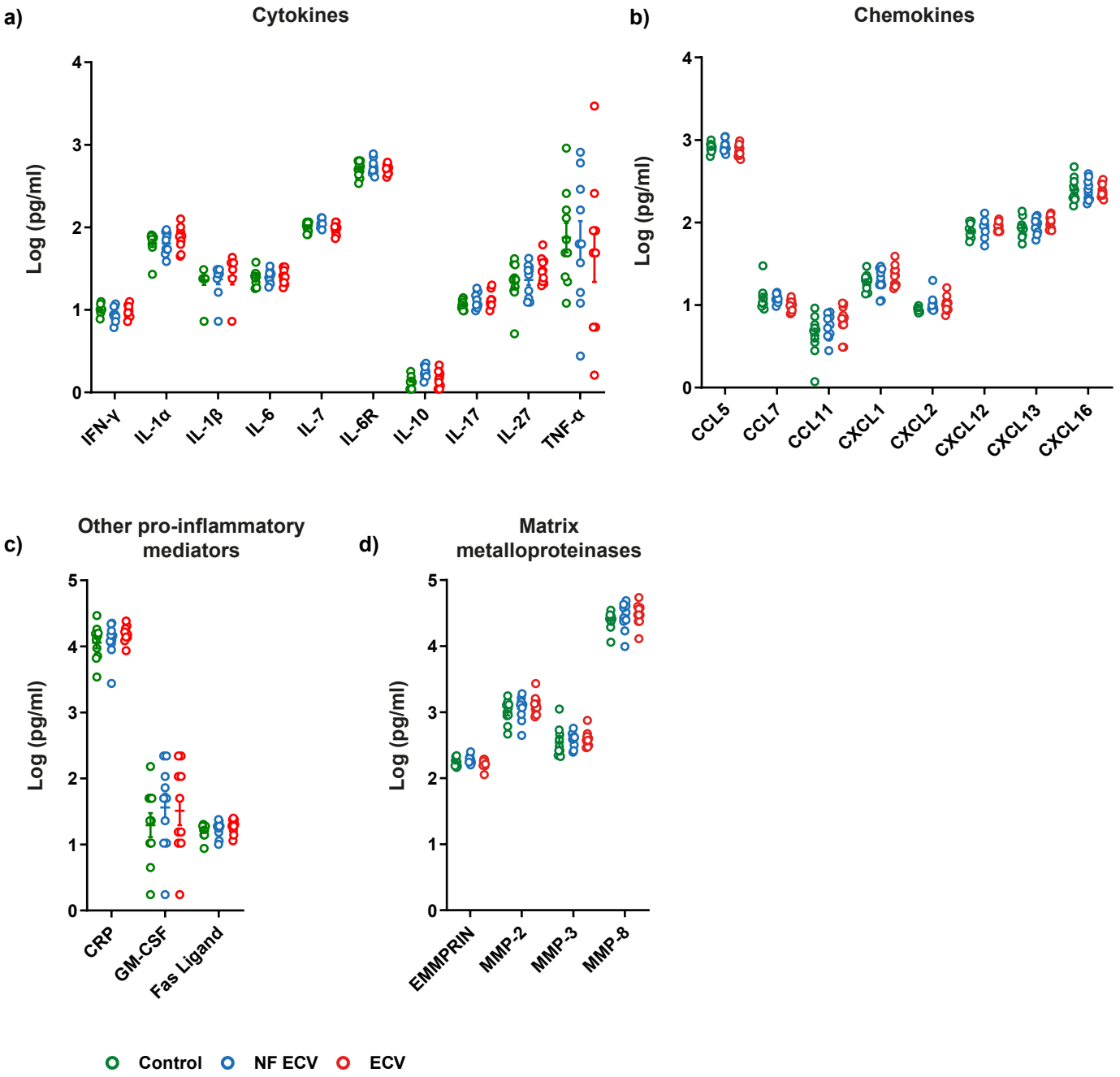

Supplementary Figure 7. Multiplex analysis of bronchoalveolar lavage fluid (BALF).
a-d) Analysis of multiplex immunoassay screening for cytokines (**a**), chemokines (**b**), other pro-inflammatory mediators (**c**) and matrix metalloproteinases (**d**) in BALF from mice exposed to either nicotine-free e-cigarette vapour (NF ECV) or nicotine-containing e-cigarette vapour (ECV) for 8 months. Control animals were treated with room air only.
Statistical analysis was performed by one-way ANOVA with Tukeys post hoc-test. n=10 mice per group. No significant differences could be observed between the Control, NF ECV and ECV groups.
Abbreviation: CCL – (C-C motif) ligands; CRP – c reactive protein; EMMPRIN – extracellular matrix metalloproteinase inducer; GF - CSF – granulocyte-macrophage colony-stimulating factor; IL – Interleukin; IFN-γ – interferon gamma; MMP – matrix metalloproteinase;TNF-α - tumor necrosis factor alpha.

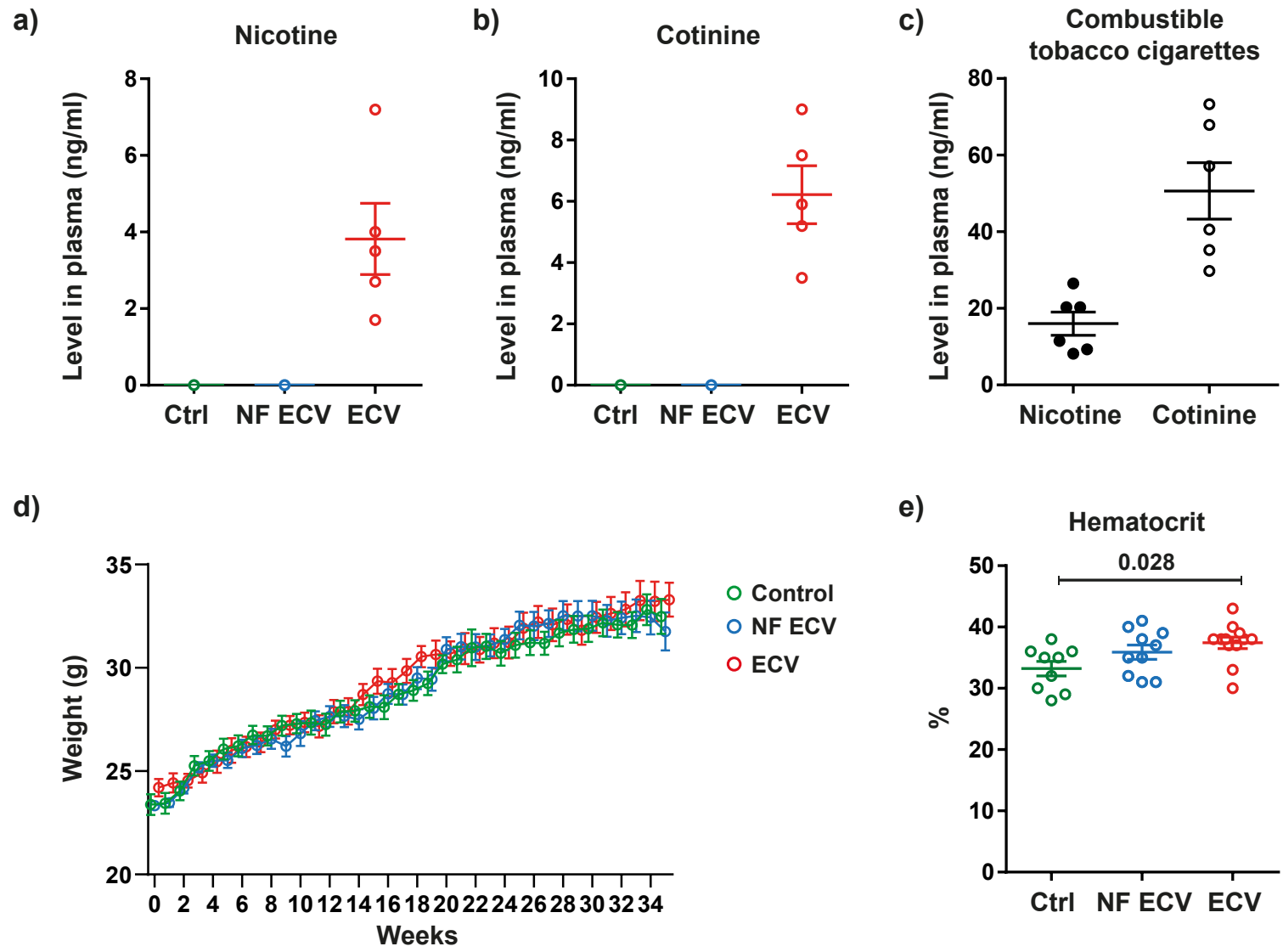

Supplementary Figure 8. Effect of long-term i*n vivo* exposure to ECV or NF ECV on nicotine, cotinine concentrations and on hematocrit.

a, b) Concentrations of nicotine (**a**) and cotinine (**b**) in the plasma of mice exposed to nicotine-free e-cigarette vapour (NF ECV) or nicotine-containing e-cigarette vapour (ECV) for 6h (n=5). **c**) Nicotine and cotinine concentration in the plasma of mice exposed to conventional CS for 6h (n=6). **d**) Mouse weight during the time course of exposure to NF ECV or ECV for 8 months. n=12 mice per group. **e**) Hematocrit (n=9-12) of mice exposed to NF ECV or ECV for 8 months. Control animals were treated with room air only. Statistical analysis was performed by one-way ANOVA with Tukeys post hoc-test. Data are presented as mean ± SEM.